QATAR UNIVERSITY

COLLEGE OF ENGINEERING

EVALUATION AND CALIBRATION OF DYNAMIC MODULUS PREDICTION MODELS OF ASPHALT MIXTURES FOR HOT CLIMATES

BY

AHMAD AL-TAWALBEH

A Thesis Submitted to

the College of Engineering

in Partial Fulfillment of the Requirements for the Degree of

Master of Science in Civil Engineering

January 2023

COMMITTEE PAGE

The members of the Committee approve the Thesis of
Ahmad Al-Tawalbeh defended on 05/01/2023.

Prof. Okan Sirin
Thesis Supervisor

Dr. Wael AlHajyaseen
Committee Member

Prof. Mostafa Elseifi
Committee Member

Approved:

Khalid Kamal Naji, Dean, College of Engineering

ABSTRACT

AL-TAWALBEH, AHMAD, M., Masters : January : [2023],
Masters of Science in Civil Engineering

Title: **Evaluation and Calibration of Dynamic Modulus Prediction Models of Asphalt Mixtures for Hot Climates**

Supervisor of Thesis: Okan Sirin

The dynamic modulus (E^*) of asphalt mixtures is considered a primary entry in Mechanistic-Empirical (ME) pavement design and analysis. Various models have been published and aimed to estimate the modulus on the basis of the mixture volumetrics and material features. This study aims to review four commonly incorporated dynamic modulus prediction models of Hirsch, Alkhateeb, Witzack 1-37A, Witzack 1-40D and validate and calibrate Hirsch and Alkhateeb models for use in Qatar. Based on the study outcomes, the Hirsch model showed a high prediction accuracy of asphalt mixture moduli before calibration with a coefficient of determination (R^2) of 87.2% between predicted and measured values. This R^2 value is improved after calibration to 89.2%. Alkhateeb model, on the other hand, had a R^2 of 70.8% before calibration, which also improved to 89.2% after calibration. Based on the study results, it is recommended to use the calibrated Hirsch or Alkhateeb model in Qatar instead of the uncalibrated version of the models. The moduli predicted by the Hirsch model before and after calibration were employed in this study to perform a mechanistic-empirical analysis of typical pavement structures in Qatar. According to the findings, the percent change in the predicted fatigue due to the use of the calibrated Hirsch model reached more than 50% with an average value of 17.33%, while the percent change in rutting reached 14% with an average value of 3.65%. These results highlight the importance of using locally calibrated models to improve dynamic modulus predictions performance.

DEDICATION

This work is devoted to my parents, siblings, and beloved ones. This work is also dedicated to

Arab World countries, the heart of the desert.

ACKNOWLEDGMENT

Great thanks to Allah (swt) for granting me this opportunity and experience throughout my life, and may the peace and blessings be on our Prophet Muhammad (peace be upon him).

I am grateful to Prof. Okan Sirin for all the great support, efforts, and time throughout this thesis. Being a humble advisor is what the students need to love their majors and work.

I also want to thank Prof. Eyad Masad, Dr. Mohammad Sadeq, Dr. Haisam Sebaaly, and Dr. Lakshmi Roja for their efforts and assistance in providing support, information, and advice.

Finally, my gratitude never faded to my employers, Seero Engineering Consulting and AECOM Middle East Limited, for collaborating with me.

TABLE OF CONTENT

LIST OF TABLES

LIST OF FIGURES

CHAPTER 1: INTRODUCTION

Overview

Asphalt mixture dynamic modulus (E^*) is one of the main factors in pavement design, especially in the mechanistic-empirical analysis and design method and estimating the layer coefficient of American Association of State Highway and Transportation Officials (AASHTO, 1993) empirical design method (Sakhaeifar et al., 2015). Due to this importance, laboratory testing is needed to characterize this parameter to provide the designer with flexibility in the material selection. However, characterizing the mixture would face multiple difficulties and determinants, such as having different sources of aggregate properties and gradation, having multi-types of asphalt binders, and the need for a large testing matrix that is not available at the design stage of the road. In order to overcome these difficulties, researchers come up with prediction models that forecast the mixture based on asphalt mixture volumetrics and asphalt binder properties such as Complex Modulus (G^*). These prediction models are generally validated based on conventional mixtures of local materials and are not aimed to be generalized for all types of materials and mixtures (B. Zhang et al., 2019) (Apeagyei, 2011). Based on the literature, Hirsch, Witzack 1-37A (1999), Witzack 1-40D (2006), and Alkhateeb dynamic modulus prediction models are the most popular models studied and applied in practice among many prediction models developed around the world and considered as a proofed concept. However, these models vary in development technique, testing matrix, and calibration methods which result in different prediction performances due to a variety of material characteristics and mixture volumetrics from one region to another (Abu Abdo, 2012) (Ceylan, Schwartz, et al., 2009) (Mateosa & Soares, 2015).

Hirsch model (Christensen et al., 2003) is developed based on the mixture rule. It was considered in the early stages as a tool to define the sensitivity of volumetrics and their effect on the dynamic modulus (C. Zhang et al., 2017). As the Hirsch model relies on mechanistic concepts and regression results, it is considered a semi-empirical model and reduces the inputs compared to the entirely empirical models such as Witzack model (M Kim, 2010). However, the empirical part of the Hirsch model was built based on the conventional mixtures dataset resulting in questionable prediction performance of the model for the new modified type of mixtures that developed for other climatic conditions.

Witzack models rely on conventional multivariate regression analysis of a large dataset of laboratory testing results (Ceylan & Kim, 2007). These models were revised and developed through the last decades to improve their prediction performance for several mixes. First, a popular version was developed in 1999 and known as 1-37A Witzack Model, and then it was reviewed in 2006 and known as Witzack 1-40D (Yousefdoost et al., 2013). In the Witzack 1-40D model, the 1-37A version has been modified by widening the original dataset and introducing the complex modulus (G^*) and the phase angle (δ) instead of the viscosity to include the loading frequency effect on the modulus (J. Bari & Witczak, 2006). Several researchers demonstrated that the 1-40D version has a good prediction performance (Ceylan, Schwartz, et al., 2009) (Yousefdoost et al., 2013) (J. Bari & Witczak, 2006). On the contrary, other studies show that the 1-40D Witzack model yields highly biased predictions (Khattab et al., 2014) (Andrei et al., 1999). Even though Witzack 1-40D is the latest model, several studies proved that Witzack 1-37A has better performance (Khattab et al., 2014) (Solatifar, 2020) (Robbins & Timm, 2011).

Alkhateeb Model defined the functional rheology of the asphalt layer as a combination of three phases of a parallel performance (Al-Khateeb et al., 2006). The research dataset included modified and unmodified asphalt mixtures with a wide range of performance grades (Al-Khateeb et al., 2006). Multiple studies showed that the Alkhateeb model resulted in biased prediction at low temperatures (Yousefdoost et al., 2013) (Far et al., 2009).

Problem Statement

Qatar has witnessed exponential growth in all infrastructure sectors and broad expansion in road networks in the past decade. The need to provide value-engineered and sustainable pavement structures has become a priority during this development. In Qatar, and to predict the dynamic modulus, Qatar Highway Design Manual (QHDM) (MOTC, 2015) and Interim Advice Note No. 101 (Public Work Authority, 2016) of the Public Works Authority (PWA) of Qatar have recommended using the Hirsch model without referring to a validation study. As this model was formed based on the USA mixtures (Christensen et al., 2003), the prediction performance of the Hirsch model of Qatar-based mixtures requires further verification and possibly recalibration in light of comparative study with other available models.

Qatar Climate

The climate condition is an essential input in determining the properties of pavement materials. Qatar has a hot climate with high humidity levels during the summer. According to the Qatar Meteorology Department, Doha has a low average annual rainfall precipitation of 79mm(QMD, n.d.-a). Figure 1 shows the climatic temperature in Qatar for the period 1962 to 2013 collected in Doha city station (QMD, n.d.-b)

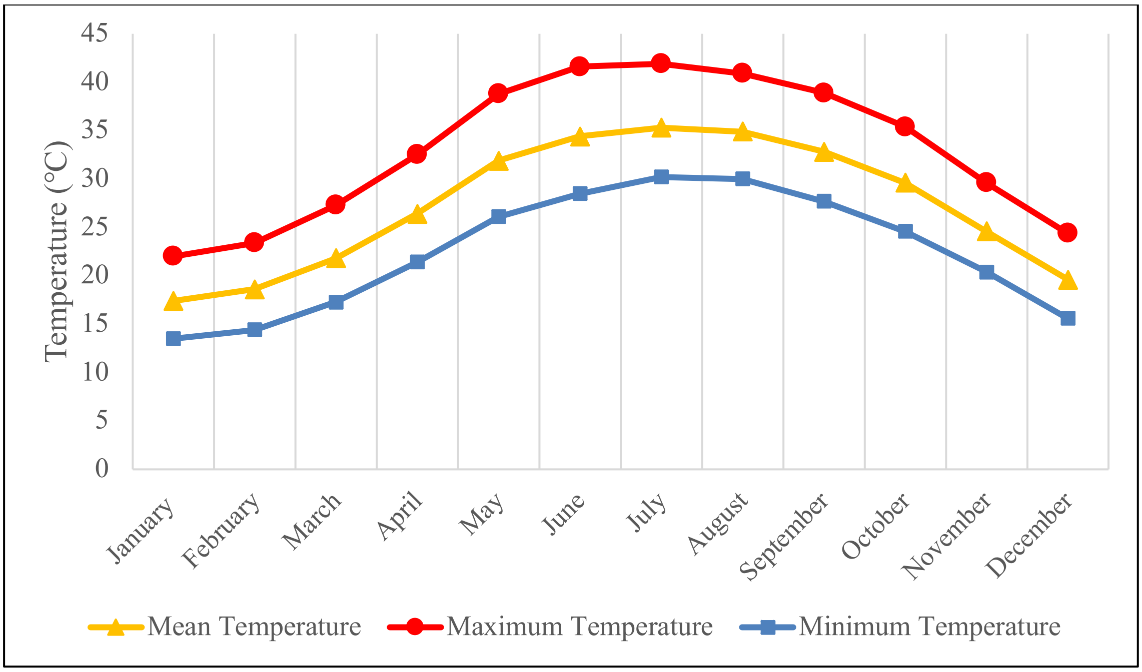

Figure 1. Climatic Temperature Normals in Qatar for the period 1962 to 2013 (Qatar Meteorology Department: Doha Station)

There is no significant deviation in the overall terrain and environment of the State of Qatar; thus, the data collected from the Doha station represents the entire country's climate. Figure 1 shows that the lowest temperature throughout the year is 13.5 °C. This explains that the State of Qatar does not experience air temperatures of 4 or 5 °C, which are typically used in dynamic modulus testing to construct the master curve.

Objectives of the Study

This study aims to:

- Select the usable models in Qatar after reviewing the Hirsch, Witzack 1-37A (1999), Witzack 1-40D (2006), and Alkhateeb dynamic modulus prediction models.

- Conduct validation and calibration for the selected models based on local materials and testing practices.

- Evaluate the advantage of the calibration on the predicted functional performance of Qatar pavement structures.

Report Outline

The thesis contains five chapters. For ease of understanding, each chapter has an introduction that explains the chapter's content and presents the expected information. The chapters contents are briefly described below.

Chapter 1: Introduction

Chapter 1 of the thesis serves as a quick introduction and outlines its goal in light of the issue statement. This chapter also includes a description of the report's outline and the study's objectives.

Chapter 2: Literature Review

Chapter 2 offers an in-depth review of the Hirsch, Witzack 1-37A (1999), Witzack 1-40D (2006), and Alkhateeb dynamic modulus prediction models prediction bases, prediction performance, calibration techniques, limitations, and the latest technologies used to build dynamic modulus prediction models and highlight future developments needed to achieve better prediction performance. This chapter reviews sensitivity studies for the effect of dynamic modulus on the predicted functional operation of pavement structures. In the end, two prediction models have been chosen for the validation and the calibration based on their inputs after eliminating the other two reviewed models.

Chapter 3: Research Methodology and Data Collection

Chapter 3 describes the research methodology developed to accomplish the targeted objectives. Also, the chapter presents the collected data and explains the calibration technique considered in this study. Lastly, the chapter shows the statistical measures considered to assess the results.

Chapter 4: Results and Discussion

Chapter 4 presents the validation and calibration results in statistical terms, discusses them, and compares them with the reviewed literature. Also, the chapter presents the sensitivity analysis results of the Hirsch and Alkhateeb models. In the end, the chapter shows the result of the functional performance testing of Qatar pavement structures before and after calibration to highlight the importance of the conducted calibration.

Chapter 5: Conclusion and Recommendations

Chapter 5 concludes this study's results and interconnects the outcomes with the study objectives. Also, the chapter includes recommendations that would be considered in future studies of dynamic modulus prediction models to improve the results.

CHAPTER 2: LITERATURE REVIEW

Introduction

Based on the above introduction, it is noticed that the evaluation studies for the four dynamic modulus prediction models resulted in contradicting results regarding the prediction performance. Therefore, this section gives a state-of-the-art review of the Hirsch, Witzack 1-37A (1999), Witzack 1-40D (2006), and Alkhateeb dynamic modulus prediction models to define the prediction bases, prediction performance, calibration techniques, limitations, and the latest technologies used to build dynamic modulus prediction models and highlight future developments needed to achieve better prediction performance. Also, this section reviews sensitivity studies on the dynamic modulus effect on the predicted functional performance of pavement structures and concludes the outcomes.

Models Prediction Bases

This section presents the Hirsch, Witzack 1-37A (1999), Witzack 1-40D (2006), and Alkhateeb prediction models prediction bases found in the literature. The section presents the theory behind each model and the dataset details that were considered to develop it.

Hirsch Model

The Hirsch model constructed by (Christensen et al., 2003) is among the most well-liked prediction models for asphalt layers modulus. This model can be categorized as a semi-empirical model that is rheologically developed based on Burger's model, which considers a synthesis of two mechanical responses for the material, parallel and series, as shown in Figure 2 (Huang, 2004)(Elseifi et al., 2002).

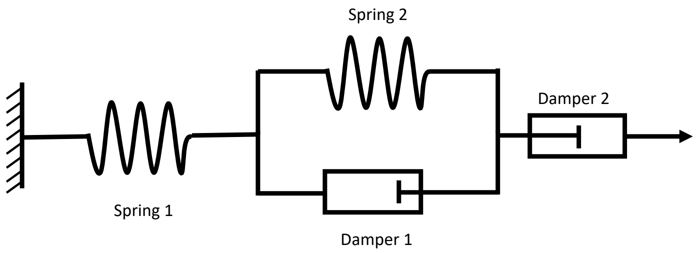

Figure 2. Burger's Model Concept Diagram

The parallel and series performance of the asphalt mixture is represented in Equations (1) and (2), respectively (Shu & Huang, 2008).

$$E_p = E_1V_1 + E_2V_2 \tag{1}$$

$$\frac{1}{E_s} = \frac{V_1}{E_1} + \frac{V_2}{E_2} \tag{2}$$

Where:

E_p = Parallel performance modulus of the material
E_s = Series performance modulus of the material
E_1 and E_2 = Modulus of each material
V_1 and V_2 = Volume of each material in the mixture

Equation (3) represents the asphalt mixture modulus based on Burger's model (C. Zhang et al., 2017).

$$|E^*|_m = x\left(E_1V_1 + E_2V_2\right) + (1-x)\left(\frac{V_1}{E_1} + \frac{V_2}{E_2}\right)^{-1} \tag{3}$$

Where:

x = Parallel mechanical response ratio
$|E^*|_m$ = Asphalt mixture dynamic modulus

It is found that Hirsch Model has different versions compared with each other in the literature. (C. Zhang et al., 2017) found that the following version represented in Equations (4) and (5), known as an alternate, is the most accurate model and commonly referred to as Hirsch Model (K. L. Roja et al., 2020).

$$|E^*|_m = Pc\left[4{,}200{,}000\left(1-\frac{VMA}{100}\right)+3|G^*|_b\left(\frac{VFA*VMA}{10{,}000}\right)\right]+ (1-Pc)\left[\frac{1-\frac{VMA}{100}}{4{,}200{,}000}+\frac{VMA}{3VFA\,|G^*|_b}\right]^{-1} \tag{4}$$

Where:

$$Pc = \frac{\left(20+\frac{VFA*\ 3|G^*|_b}{VMA}\right)^{0.58}}{650+\left(\frac{VFA*3|G^*|_b}{VMA}\right)^{0.58}} \tag{5}$$

Where:

$|E^*|_m$= Predicted asphalt mixture dynamic modulus (psi)
VFA = Voids filled with asphalt (%)
VMA = Voids in the mineral aggregate (%)
$|G^*|_b$ = Complex modulus of binder (psi)

The constants (20, 0.58, and 650) are fitting parameters obtained from regression analysis and fitting with measured moduli of asphalt mixtures (C. Zhang et al., 2017). The regression constant (4,200,000) is an assumed aggregate young's modulus (in psi). The constant (3) multiplied with the $|G^*|_b$ is obtained by assuming that asphalt is an incompressible material with a Poisson's ratio (v) of 0.5 substituted in the elastic modulus (E) equation: $\mathrm{E} = 2\,(1+v)|G^*|_b$, where ($|G^*|_b$) is binder modulus (C. Zhang et al., 2017).

Hirsch model was created using a dataset collected from several projects in the US. A summary of the Hirsch model dataset details is presented in Table 1 (Christensen et al., 2003). Hirsch model dataset physical features are exhibited in Table 2 (Christensen et al., 2003).

Table 1. Summary of Hirsch Model Dataset Details

Factor \ Source Project	FHWA ALF*	West Track	MN/Road	Variants Totals
Binders	SBS Modified and PE- modified	PG 64-22	120/150-Pen	8
Mix Design Method	Marshall AC-5, 10, 20	Superpave	Marshall AC-20	2
Aggregate Size and Gradation	19mm Dense and 37.5mm Fine	19mm Fine and 19mm Coarse	9.5mm Fine	5
Number of Asphalt Mixes	7	6	5	18
No. of Data Point	78	69	59	206

* ALF: Accelerated Load Facility

Table 2. Hirsch Model Dataset Physical Properties

Criteria	**Value**
Air Voids (%)	5.6 to 12.2
VMA (%)	13.7 to 21.6
VFB (%)	38.7 to 68
Loading Frequency (Hz)	0.1 and 5
Dynamic Modulus (MPa)	183 to 20,900
Complex Shear Modulus (MPa)	20 to 3,880
Temperature (°C)	4, 21 and 38
Phase Angle (degrees)	8 to 61

Witzack 1-37A Model (1999)

This empirical model was developed by Andrei Witzack et al. by collecting a database consisting of 205 asphalt mixtures tested at 2750 test points (C. Zhang et al., 2017). Shook and Kalas originally developed the model in 1969, which was modified by Fonseca and Witzack in 1996 (Li et al., 2012). A database contains 1430 data points obtained based on 149 conventional asphalt mixes initially utilized in the Fonseca and Witzack model, as well as a further 1320 test points from 56 asphalt mixtures the contains 34 mixtures have an enhanced asphalt binder, which was used to create the Witzack 1-37A model. The model inputs include volumetric characteristics, asphalt mix grading, viscosity, and frequency. In Equation (6), the Witzack 1-37A model is displayed (Andrei et al., 1999).

$$Log\ |E^*|_m = -1.249937 + 0.029232.p_{200} - 0.001767\ .(p_{200})^2 - 0.002841.p_4$$
$$-0.058097.V_a - 0.802208.\frac{V_{beff}}{(V_{beff} - V_a)}$$
$$+\frac{3.871977 - 0.0021.p_4 + 0.003958.p_{38} - 0.000017.(p_{38})^2 + 0.005470.p_{34}}{1 + e^{(-0.603313 - 0.313551.log(f) - 0.393532.log(\eta))}} \quad (6)$$

Where:

$\vert E^*\vert_m$ =	Predicted Dynamic Modulus, in 0.72 MPa (105 psi)
p_{200} =	% Passing the sieve No.200
p_4 =	% Retained on sieve No. 4
V_a =	% Air voids
p_{38} =	% Retained on the 9.5 mm (3/8-inch) sieve by total aggregate weight (cumulative)
V_{beff} =	% Effective bitumen content, by volume
p_{34} =	% Retained on the sieve sized 19 mm (3/4-inch)
f=	Loading frequency (Hz)
Ƞ =	Bitumen viscosity

A summary of the Witzack 1-37A set of data is demonstrated in Table 3 (Garcia & Thompson, 2007).

Table 3. Summary of Witzack 1-37A Dataset Details

Criteria	**Dataset**
Frequency	0.1 to 25 Hz
Binder Types	9 Unmodified, 14 Modified
Temperature	-17.7 to 54.4 °C
Asphalt Mixtures	34 with modified binder, 171 with unmodified binder
Aggregate	39 grading type
Specimen Aging	Un-aged

Witzack 1-40D Model (2006)

The Witzack 1-40D model revised the previous Witzack 1-37A by expanding the database and introducing the G^* and δ instead of viscosity. This model was calibrated subject to 7400 modulus test points resulting from testing 346 Hot Mix Asphalt (HMA). The new data when compared with the Witzack 1-37A model data added aged and un-aged material of wider variety in the aggregate gradation, binder types, and mixture types (modified and unmodified) (Javed Bari et al., 2006).

The 1-40D model kept the same structure as the Witzack 1-37A model, but G^* and δ were embedded in the equation (Robbins & Timm, 2011). The model is represented by Equation (7) (J. Bari & Witczak, 2006).

$$
\begin{aligned}
Log\,|E^*|_m = {} & -0.349 + 0.754(|G_b^*|^{-0.0052})\, x\, (6.65 - 0.032p_{200} \\
& + 0.0027{p_{200}}^2 + 0.011p_4 - 0.0001{p_4}^2 + 0.006p_{38} \\
& -0.00014{p_{38}}^2 - 0.08V_a - 1.06\left(\frac{V_{beff}}{V_a + V_{beff}}\right)) \\
& + \frac{2.56 + 0.03\,V_a + 0.71\left(\frac{V_{beff}}{V_a + V_{beff}}\right) + 0.012p_{38} - 0.0001{p_{38}}^2 - 0.01p_{34}}{1 + e^{(-0.7814 - 0.578585\log|G^*|_b + 0.8834 log\delta_b)}}
\end{aligned} \tag{7}
$$

Where:

$|G^*|_b$ = Complex modulus of the binder (in psi)

δ_b = Phase angle of the binder (in degrees)

Alkhateeb Model

In addition to the Hirsch model, the Alkhateeb model (Al-Khateeb et al., 2006) has been applied in the practice due to its small number of inputs needed to predict the E^*. The model was constructed based on the rule of mixtures considering a three-component system of binder, aggregate, and air voids. (Al-Khateeb et al., 2006) determined the calibration parameters using mixtures from the State of Virginia in the USA. The set of mixtures included aging effect and modified binders. Equation (8) represents the Alkhateeb model (Al-Khateeb et al., 2006).

$$|E^*|_m = 3\left(\frac{100 - VMA}{100}\right)\left(\frac{\left(90 + 1.45\frac{|G^*|_b}{VMA}\right)^{0.66}}{1100 + \left(0.13\frac{|G^*|_b}{VMA}\right)^{0.66}}\right)|G^*|_g \quad (8)$$

Where:

$|G^*|_g$ = Binder glassy state shear modulus in Pa (assumed as 10^9 Pa)

VFA = Fraction of aggregate voids filled with asphalt (%)

VMA = Voids in the mineral aggregate (%)

$|G^*|_b$ = Binder complex modulus (asphalt) (psi)

The model was developed based on several material resources, production techniques, and binder types. Table 4 shows the Alkhateeb model dataset details, while Table 5 shows the physical properties of the Alkhateeb model dataset (Al-Khateeb et al., 2006).

Table 4. Summary of Alkhateeb Model Dataset Details

Mixture Production Types	**Compaction Types**	**Binder Types**
Laboratory Produced	Laboratory Compaction	PG 70-28 air blown
Plant Produced	Field Compaction	PG 70-22 unmodified
Field Cores		PG 70-28 modified by polymers
		PG 76-28 modified by crumb rubber
		PG 70-34 modified by polymers

Table 5. Alkhateeb Model Dataset Physical Parameters

Mixture Properties		**Grading**	
Sand Equivalent (%)	75	Size (mm)	Percent Passing
Bulk Saturated Surface Dry Gravity (t/m3)	2.965	37.5	100
NMAS (mm)	12.5	9.5	84.6
Apparent Specific Gravity (t/m3)	3.001	12.5	93.6
LPLC* Binder Content (%)	5.3	4.75	56.7
LPLC* and PPLC** Compaction	Gyratory	2.36	34.9
Specimen Cylinder Size(mm)	100 x 150	1.18	24.8
Test Temperature (°C)	4, 9, 31, 46, 58	0.6	18.2
Absorption (%)	0.6	0.3	13.1
Air Voids - Targeted (%)	7±0.5	0.15	9.3
Test Frequency (Hz)	0.1, 0.5, 1, 5, 10		
Bulk Dry Specific Gravity (t/m3)	2.947		

* LPLC: Lab Produced – Lab Compacted

** PPLC: Plant Produced – Lab Compacted

Models Comparison Summary

Based on the review conducted in the previous sections, the comparative summary of the four models is presented in Table 6.

Table 6. Comparison of the four reviewed models

Criterion	**Hirsch Model**	**Witzack 1-37A model**	**Witzack 1-40D model**	**Alkhateeb model**
Prediction Type	Semi-empirical (C. Zhang et al., 2017)	Empirical (Ceylan & Kim, 2007), (Andrei et al., 1999)	Empirical (Ceylan & Kim, 2007), (Andrei et al., 1999)	Semi-empirical (Al-Khateeb et al., 2006)
Number of Test points	206 (Christensen et al., 2003)	2,750 (Yousefdoost et al., 2013), (Andrei et al., 1999)	7400 (Ceylan & Kim, 2007), (Andrei et al., 1999)	150 (Al-Khateeb et al., 2006)
Number of Mixtures	18 (Christensen et al., 2003)	205 (Yousefdoost et al., 2013), (Andrei et al., 1999)	346 (Ceylan & Kim, 2007), (Andrei et al., 1999)	6 (Al-Khateeb et al., 2006)
Type of Binders	2 Unmodified and 2 Modified (Christensen et al., 2003)	Unmodified and Modified (Yousefdoost et al., 2013), (Andrei et al., 1999)	Unmodified and Modified (Andrei et al., 1999)	6 Types of Modified and Unmodified (Yousefdoost et al., 2013), (Al-Khateeb et al., 2006)
Aggregate Gradation	1 Dense, 3 Fine, and 1 Coarse (Christensen et al., 2003)	39 Types (Yousefdoost et al., 2013), (Andrei et al., 1999)	Gap, Open, and Dense (Andrei et al., 1999)	1 Dense (Yousefdoost et al., 2013), (Al-Khateeb et al., 2006)
Aging	Aged	Un-aged (Yousefdoost et al., 2013), (Andrei et al., 1999)	Aged and Un-aged (Andrei et al., 1999)	Aged (Yousefdoost et al., 2013), (Al-Khateeb et al., 2006)
Assumed Rheology	Two Phases in parallel and series (Christensen et al., 2003)	Not Applicable	Not Applicable	Three phases in parallel (Al-Khateeb et al., 2006)

Models Performance Comparison

As the above-mentioned prediction models relied on different techniques and datasets, the prediction performance varies from one region to another due to climatic and material differences. (C. Zhang et al., 2017) study evaluated the performance of the Hirsch model, the Witzack 1-40D model, and the modified Hirsch model proposed through the study. The study also aimed to revise the Hirsch model by introducing the mixture's rule in addition to considering the elastic and viscoelastic properties. The study went through a rheological review for the Hirsch model and found that there are three sources of error in the model; (1) the model always assumes the aggregate modulus as a regression constant of 4,200,000 psi; (2) the model has been derived based on the assumption that asphalt mixture is elastic material so dynamic modulus was represented as $E^* = 2(1 + v)|G^*|_b$; (3) the asphalt is assumed as incompressible with poisons ratio of 0.5. At first, the researchers conducted a sensitivity analysis to examine the influence of aggregate modulus on the forecasting performance of the Hirsch model by substituting the modulus of limestone, basalt, and tuff instead of the utilized 4,200,000 regression constant in the model and comparing it with a control limestone asphalt mixture modulus. The analysis showed that using a specific aggregate modulus is necessary due to the significant difference in the prediction when using a regression constant of 4,200,000. Figure 3 explains the aggregate modulus effect on predicted dynamic modulus based on the study outcomes (C. Zhang et al., 2017).

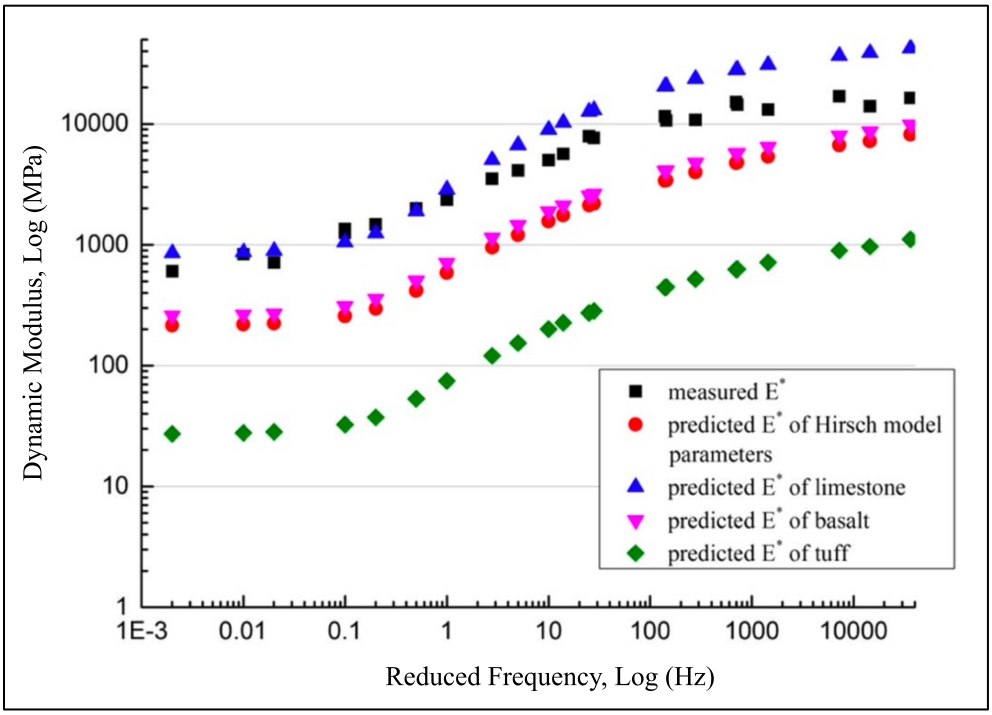

Figure 3. Measured Vs. Hirsch Predicted Mixtures Master Curve with Several Types of Aggregate

Figure 3 shows that the basalt modulus comes up in the closest prediction to the original Hirsch model values since the regression constant of 4,200,000 is close to the basalt modulus of (34,894 MPa) 5,061,000 psi (Stowe, 1969) so the prediction performance does not significantly vary. Also, the limestone resulted in the closest predicted modulus compared to the measured values since it is used in the control mixture.

(Yousefdoost et al., 2013) studied the appropriateness of the US (Alkhateeb, Hirsch, Witzack 1-37A, and Witzack 1-40D) models for Australian mixtures. In order to achieve the study goal, 28 asphalt mixtures used in Australia have been tested to define the modulus. The study concluded that the Hirsch, Witzack 1-37A (1999), and Alkhateeb models typically under-predict the dynamic modulus; meanwhile, Witzack 1-40D (2006) exaggerates the values. Bias and fitting errors were computed for each model and found high in the Hirsch, Alkhateeb, and Witzack 1-40D. The study also came up with the conclusion that all models' prediction accuracy is sensitive to temperature. The study also included sensitivity analysis to check how the asphalt mix properties affect the prediction accuracy. It was found that binder type is the most sensitive characteristic. Therefore, the conclusion was interpreted that the studied prediction models are not accurate enough to be considered for Australian asphalt mixes. Table 7 shows the Goodness-of-fit of prediction models for Australian asphalt mixes.

Table 7. Goodness-of-fit of Prediction Models for Australian Asphalt Mixes

Statistics	**Criteria**	**1-37A**	**1-40D**	**Hirsch**	**Alkhateeb**
S_e/S_y	5 °C	1.55	7.9	2.84	2.85
	20 °C	0.86	2.29	1.34	1.26
	35 °C	0.43	0.38	0.72	0.57
	50 °C	1	0.39	0.53	0.48
	Overall	0.49	2.29	0.88	0.87
R^2	5 °C	-134.00%	-5998.00%	-702.00%	-709.00%
	20 °C	29.00%	-412.00%	-78.00%	-58.00%
	35 °C	82.00%	86.00%	49.00%	68.00%
	50 °C	2.00%	85.00%	73.00%	77.00%
	Overall	76.00%	-419.00%	1300.00%	24.00%
Other Statistics	SSE	1.75E+10	3.79E+11	5.59E+10	5.51E+10
	Average $\|E^*_p\|$	5953	16555	3812	4000
	Average Error	-2007	8595	-4147	-3959
	Slope	0.618	2.688	0.342	0.332
	Intercept	1030.8	-4837.5	1090	1357.8
	Rating	Good	Very Poor	Poor	Poor

(Far et al., 2009) conducted a study to evolve an Artificial Neural Network (ANN) dynamic modulus prediction model and evaluated Alkhateeb, Hirsch, Witzack 1-37A, and Witzack 1-40D models. The study concluded that the Alkhateeb model has a significant bias at low temperatures compared to 1-40D Witzack and the Hirsch models. In addition, the study modified all four models to improve the prediction performance. It was concluded that the newly modified Witzack and Hirsch models result in significant bias at high temperatures and low sensitivity of the two models to volumetric parameters.

(Solatifar, 2020) conducted a study to compare the performance of six dynamic modulus prediction models (Hirsch, Modified Witzack, Witzack, Alkhateeb, Global, and Simplified Global). The study includes a published database conducted by the University of Maryland. The testing consists of a broad extent of frequencies and temperatures. To evaluate the prediction performance of the studied models, the study considered two Measures for Effectiveness (MOE), which are goodness-of-fit and bias. The study concluded that the best prediction performance is arranged as Witzack 1-37A, Simplified Global, Global, Hirsch, Alkhateeb, and Modified Witzack 1-40D. The study highlighted that the Witzack 1-37A model has the best prediction performance because it was developed based on the same testing database utilized in this study. Although calibration is necessary, the study concluded that all models could be considered in the design and analysis process.

To establish the use of AASHTOWare software for the Pavement Mechanistic-Empirical (ME) design method in Saudi Arabia, (Khattab et al., 2014) analyzed Witzack 1-37A and 1-40D dynamic modulus prediction models. The modulus was measured for 25 different local mixtures. The results indicated that temperature and binder type impacted how well the two models worked. According to the data, MEPDG Level 3 binder inputs and the 1-37A Witzack model had the highest prediction performance and lowest biased prediction.

(Robbins & Timm, 2011) conducted a study evaluating Hirsch, Witzack 1-37A, and Witzack 1-40D on asphalt mixtures in the southeastern United States by testing 18

HMA. The Witzack model found to had the largest deviations from the measurements with overestimating E^* by about 61%.

Models Calibration Techniques

Due to the importance of Dynamic Modulus (E^*) prediction models in practical fields, several researchers focused on developing a methodology to calibrate the models (Goh et al., 2010). (C. Zhang et al., 2017), proposed to calibrate the Hirsch model with two major changes: (1) introducing Burger's model to describe binder viscoelastic properties and (2) considering design-specific aggregate elastic modulus instead of the regression constant. The study came up with a modified Hirsch model that includes the δ of the mix. It was concluded that the modified Hirsch model in this study provides higher accuracy prediction than the original Hirsch and 1-40D Witzack models. In addition, it was found that the prediction performance is sensitive to the δ value.

(Robbins & Timm, 2011) proposed the Hirsch model calibration methodology by substituting the actual aggregate modulus instead of the regression constant of 4,200,000. The used aggregate modulus considered in the mix has a modulus of 3,040,500 psi. In addition, the research proposed to use an error minimization tool in excel to find new regression factors instead of (20, 650, 0.58, 3). The calibration shows an improvement of 1.4% R^2 for the Hirsch model prediction, which was considered as minor improvement.

(Shen et al., 2013) proposed two calibration techniques for the Hirsch model based on Washington DC asphalt mixes using 42 samples. The first calibration technique considered replacing the 4,200,000 regression constant with an aggregate modulus of 4,800,000 psi and using error minimization to replace the regression coefficient (20, 650, and 0.58) with new values. The study resulted in a new regression coefficient of (0.2, 600, and 0.56), respectively. It was concluded that the quality of the predictions improved but overestimated the modulus at high testing temperatures. In the second technique, the research proposed using asphalt mastic properties to calibrate the Hirsch model. The study suggested a factor of 68,947 MP (10,000,000 psi) instead of 4,200,000 regression constant and considered using mastic complex modulus ($G_m{}^*$) instead of binder G^* and replacing the regression factors (650 and 0.58) with (10,000 and 0.67), respectively. Figure 4 shows the newly improved prediction performance based on the second technique (Shen et al., 2013).

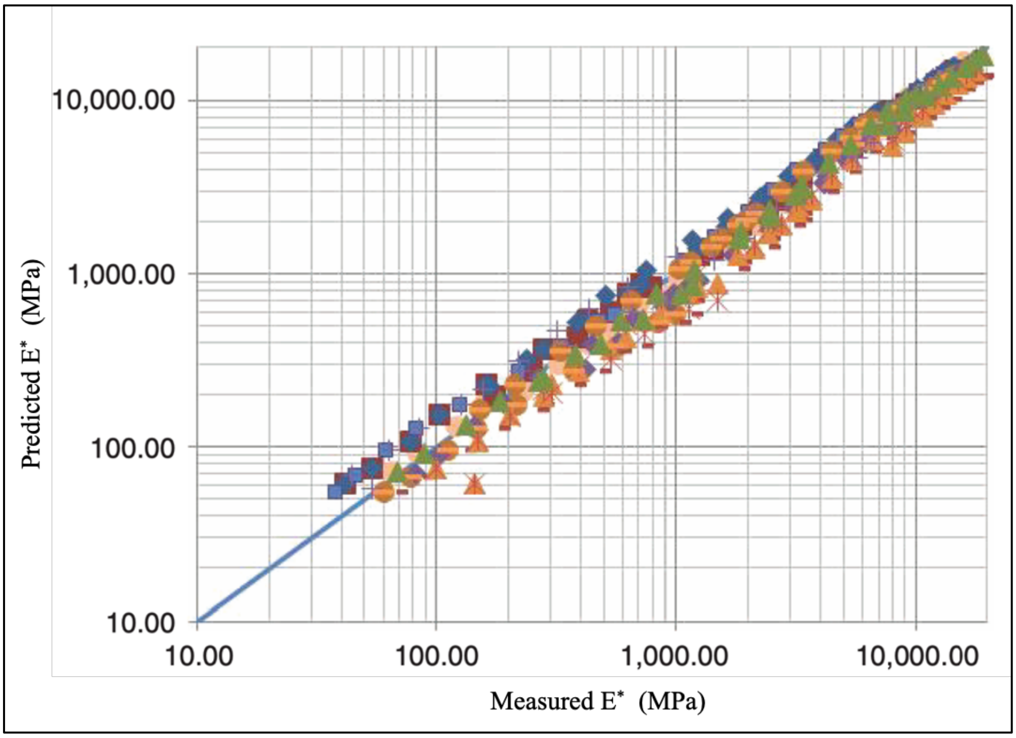

Figure 4. Predicted and Measured E^* based on Modified Hirsch Model of Shen et al. study

The trend of the predicted vs. measured E^* is going around the line of equality, and the performance appears consistent. Unfortunately, the published article did not present the statistical improvement of the prediction in the article.

Recent Developments and Future

New dynamic modulus prediction models have been developed with innovative techniques to overcome the shortcomings of conventional models (Ceylan, Gopalakrishnan, et al., 2009). Kim (Minkyum Kim, 2009) explained that empirical and semi-empirical models for predicting dynamic elastic moduli have significant shortcomings, especially when used for mixtures that vary significantly from those used to develop and calibrate the model. In the study, a proposed and experimentally validated a differential scheme micromechanics modeling framework for HMA modulus prediction was considered. Researchers have identified material micromechanics at the level of their individual components. After developing the new model, the predicted and measured E^* have been compared and a good agreement was found with reasonable accuracy.

(Ceylan & Kim, 2007) conducted a study to develop a simple dynamic modulus prediction model with less number of independent variables in comparison to the regression-based models such as Witzack models without negatively impacting the accuracy of the prediction. The Witzack 1-40D measured E^* dataset was considered for constructing Artificial Nural Network (ANN) based models. The obtained ANN-based models were checked against the MEPDG models. It was concluded that the ANN models with a smaller number of inputs have better performance and higher accuracy than regression-based MEPDG models.

(Far et al., 2009) constructed three ANN-based models based on the inputs of Alkhateeb, Hirsch, and 1-40D Witzack models. After validation of the three models, it was concluded that all three models have a high coefficient of determination (R^2) and low bias. The ANN model with Hirsch model inputs had the best prediction for the modulus (Lu et al., 2009).

(El-Badawy et al., 2018) applied the ANN technique for dynamic modulus prediction based on 25 asphalt mixtures and considered the inputs of Hirsch, Witzack 1-37A, and Witzack 1-40D. After determining the most sensitive inputs using Global Sensitivity Analysis (GSA) and commercially available software, the ANN-based models were found to be more accurate than conventional models. The study concluded that the Hirsch model needs further aggregate characteristics inputs so, the model's accuracy will not be negatively affected.

(Moussa & Owais, 2020) developed a Deep Convolution Neural Networks (DCNNs) technique based on six convolution blocks and applied it on Witzack 1-37A and Witzack 1-40D. The study found that the developed models based on machine learning have a higher performance than conventional prediction models. In another research by the same researchers (Moussa & Owais, 2021), a prediction model-based Deep Residual Neural Networks (DRNNs) technique was developed based on comparing 8191 combinations of inputs. The study showed that the DRNNs model outperformed the conventional Witzack 1-37A, Witzack 1-40D, and Hirsch prediction models.

Dynamic Modulus Effect on Pavement Performance Predictions

(Cooper et al., 2015) performed research to define dynamic modulus impact on pavement performance predictions. For this purpose, ten asphalt mixtures moduli were obtained at the design, production, and construction stages. Consequently, Mechanistic-Empirical (ME) pavement analysis was conducted using AASHTOWare. The analysis showed that rutting distresses were sensitive to the modulus value. Moreover, it was found that the predicted alligator cracking between plant-produced laboratory-compacted (PL) samples and field cores of the same mixture reached a 60% difference due to changes in the modulus value.

(Cheng et al., 2021) studied the sensitivity of the loading wave types on the modulus value and, consequently, on the pavement layers distresses. The study considered three loading modes and found that field strain responses differ significantly by changing the modulus inputs within the MEPDG method.

Summary and Conclusion

Based on the above-presented literature review, it was found that all four models rely on modified and unmodified binders with datasets limited to a specific area region. In terms of models' performance, it was concluded that the models have varying performances based on the temperature, frequency, and country of application.

This section also presented recent calibration techniques found in the literature that opens the doors to develop prediction models with better accuracy by considering the effect of high and low temperatures on prediction performance.

Based on this section, the following can be concluded:

- Error minimization technique has been used in several studies to calibrate the models.
- Witzack models have many inputs that are not usually presented in Job Mix Formulas (JMFs) in Qatar, such as viscosity and effective binder content by volume.
- Witzack models have many regression-fitting factors that would result in overfitting once error minimization is applied over the model.
- Within the Hirsch model, the regression constant of 4,200,000 replaces the aggregate young modulus. The error resulting from this constant decreases significantly if the mixture aggregate young modulus in psi unit is close to this constant.

- Artificial Neural Network (ANN) and Machine Learning (ML) techniques were adopted in several studies to replace conventional models such as Hirsch and Witzack models. However, this practice needs a comprehensive dataset and many testing points.
- The effect of climate is introduced in the reviewed validation and calibration techniques by considering local materials and mixing practices of the targeted study area.
- The literature has no general agreement on the performance of the reviewed prediction models. Every model shows varying performance based on the temperature and materials.
- The reviewed studies evaluate the models' predictive performance solely based on statistical analysis. The effect of the prediction model calibration was not interconnected with the predicted functional performance of the pavement structures, such as fatigue and rutting.

Based on the above-drawn conclusion, Witzack 1-37A and 1-40D models will be eliminated from the validation and calibration part due to high numbers of needed inputs which are usually not presented in Qatar Job Mix Formulas (JMF) (sample is attached to Appendix B), and due to a high number of fitting factors needed to compute the dynamic modulus values. Accordingly, the following sections will focus on evaluating and calibrating the Hirsch and Alkhateeb models for Qatar.

CHAPTER 3: METHODOLOGY AND DATA COLLECTION

Introduction

This chapter describes the research methodology developed to achieve the stated study objectives. The chapter also goes into the considered calibration technique and displays the data acquired for this purpose. The chapter also shows the statistical metrics and their interpretations used to evaluate the results.

Methodology

Based on the reviewed literature and the defined gap in this study area, the following methodology has been considered.

- Collecting laboratory testing points of Qatar asphalt binder and mixtures modulus covering a wide range of local materials, temperatures, and frequencies tested based on Qatar guidelines.
- Substitute binder and mixture properties in Hirsch and Alkhateeb model and find the predicted dynamic modulus.
- Compare the predicted dynamic modulus with the measured values.
- Validate both Hirsch and Alkhateeb models based on bias and goodness-of-fit measures.
- Calibrate both models by using the error minimization tool in excel software and define new fitting factors.
- Study the effect of models' calibration on the predicted performance of asphalt pavement structures used in Qatar by performing mechanistic-empirical pavement analysis.

Data Collection

The master curve equation of the binder and mixture modulus considered in this study is represented in Equation (9) (AASHTO, 2017).

$$\log|M^*| = \delta + \frac{\alpha}{1 + e^{-\beta - \gamma . \log f_r}} \tag{9}$$

Where $|M^*|$ is the modulus value of either the mixture or binder, (δ, α, β, and γ) are the fitting parameters, and f_r is the reduced frequency defined in Equation (10) (AASHTO, 2017).

$$f_r = f . a(T) \tag{10}$$

Where $a(T)$ is the temperature shift coefficient that can be calculated using Equation (11) (AASHTO, 2017).

$$\log\big(a(T)\big) = a_1\big(T^2 - T_{ref}^2\big) + a_2\big(T - T_{ref}\big) \tag{11}$$

Where (a_1 *and* a_2) are the temperature shift factors and (T *and* T_{ref}) are the actual testing temperature and curve reference temperature, respectively.

Binder master curve parameters are collected from two studies conducted in Qatar (L. K. Roja et al., 2021) (L. K. Roja et al., 2022) to find the $|G^*|_b$ that needed to predict the binder dynamic moduli in both Hirsch and Alkhateeb models at different frequencies and temperatures. The collected binder types represent the country's most common binders used in recently constructed road projects. The dataset includes an unmodified binder, Polymer Modified Binder (PMB) containing styrene-butadiene-styrene (SBS), Crumb Rubber Modified Binder (CRMB), and Reclaimed Asphalt Binder (RAB) with different mixing percentages mixed with unmodified PEN 60/70 (PG64S-22) binder. All used materials are admitted for use in Qatar. The dataset represents a wide range of Superpave PG grading. The binder types and relevant master curve coefficients are presented in Table 8.

Table 8. Binder Types and Coefficients of Binder Master Curves

Binder Type	Binder Grade	Master curve coefficients						
		δ	**α**	**β**	**ɣ**	**a_1**	**a_2**	**T_{ref} (°C)**
Unmodified	PEN 60/70*	-0.7380	8.8480	-0.0330	0.5880	0.0010	-0.1690	46.0
PMB	PG 76E-10	-0.9450	10.4730	0.0960	0.3080	0.0007	-0.1430	46.0
CRMB	PG 76E-10	1.5470	7.3020	0.5445	0.3925	0.0008	-0.1511	21.0
15% RAB	PG 70S-22	0.0514	8.3672	0.2467	0.4401	0.0007	-0.1438	46.0
25% RAB	PG 70S-16	0.7145	7.9034	0.0001	0.4414	0.0007	-0.1437	46.0
35% RAB	PG 70S-10	0.0001	9.7364	0.0001	0.3399	0.0007	-0.1437	46.0

* PEN 60/70 binder is equivalent to grade PG64-22

Besides the binder dataset, twenty asphalt mixtures master curves are collected from several studies (L. K. Roja et al., 2021) (L. K. Roja et al., 2022) (Sebaaly et al., 2020) and construction projects in Qatar. The collected data set included mixtures used in the Wearing Course (WC) and Asphalt Base Course (ABC) with 19 and 25mm Nominal Maximum Aggregate Size (NMAS), respectively. The asphalt mixtures represented the materials and designs used in Qatar and were tested based on Qatar Construction Specification (QCS), 2014 (MOE, 2014). The binder content percentage (BC%) of the collected data ranges between 3.4% - 4.3%, while the Air Void ratio (V_a) of the test specimens ranges between 5.2% - 7.0%. The master curve coefficients of the collected mixtures are presented in Table 9. The composition and volumetrics of the collected mixtures are shown in Table 10.

It is to be noted that each binder and mixture modulus master curve was constructed after conducting the testing on three replicates and finding the average value of the modulus after assuring the low variability in the modulus value between the replicates as per Qatar guidelines.

Table 9. Coefficients of Mixture Master Curves of the Study Dataset

HMA No.	Master curve coefficients δ	α	β	γ	a_1	a_2	T_{ref} (°C)
1	1.3309	3.1640	1.1334	0.3973	0.000610	-0.164685	20
2	1.8844	2.4852	1.0388	0.5557	0.000720	-0.164155	20
3	1.2225	3.1417	1.2301	0.5229	0.001994	-0.216857	20
4	-7.9430	12.8600	2.3860	0.1690	0.000831	-0.178000	21
5	-2.1850	6.9960	1.6330	0.2560	0.000737	-0.172243	20
6	-2.3190	6.9330	1.8690	0.2780	0.000899	-0.180347	20
7	-2.2800	6.8980	1.7860	0.2660	0.000948	-0.174775	20
8	-2.2210	6.8700	1.7580	0.2660	0.001050	-0.184469	20
9	-2.2280	6.7510	2.0530	0.2750	0.000920	-0.176847	20
10	-2.4620	7.0660	1.8630	0.2810	0.001206	-0.192653	20
11	-2.2700	6.9550	1.8850	0.2370	0.000952	-0.176755	20
12	-2.1560	6.8590	2.0260	0.2650	0.001154	-0.191043	20
13	-0.3760	4.9740	1.5660	0.2910	0.000510	-0.151924	20
14	-2.1410	6.7370	1.7590	0.2730	0.000720	-0.161181	20
15	-2.3330	6.8840	2.0900	0.3700	0.001066	-0.178346	20
16	-2.2560	6.8740	2.1550	0.2720	0.000691	-0.169981	20
17	4.3980	-1.8998	-0.1937	-0.5781	0.000376	-0.137171	20
18	4.3755	-2.0522	-0.6525	-0.5910	0.000664	-0.150427	20
19	4.4333	-2.2062	-0.6040	-0.4591	0.000118	-0.124096	20
20	4.4018	-1.9586	-0.7128	-0.4767	0.000263	-0.134852	20

Table 10. Mixtures Composition and Volumetrics of the Study Dataset

HMA No.	Binder Type	Binder Grade	Mixture Rule	NMAS [mm]	Aggregate Type	BC %	V_a [%]	VMA [%]	VFA [%]
1	PMB	PG76E-10	ABC	25	Gabbro	4.10	6.10	16.20	62.60
2	PMB	PG76E-10	WC	19	Gabbro	4.30	6.00	15.80	61.90
3	Unmodified	PEN60/70	ABC	25	Gabbro	3.40	6.65	15.00	55.70
4	CRMB	PG76E-10	ABC	25	Gabbro	3.90	6.70	16.10	58.40
5	Unmodified	PEN60/70	WC	19	Gabbro	3.90	6.20	15.80	60.80
6	Unmodified	PEN60/70	WC	19	Gabbro	3.80	6.50	15.90	59.10
7	Unmodified	PEN60/70	WC	19	Gabbro	3.40	6.40	14.70	56.50
8	Unmodified	PEN60/70	WC	19	Gabbro	3.60	6.50	15.50	58.10
9	Unmodified	PEN60/70	WC	19	Gabbro	3.90	6.70	16.50	59.40
10	Unmodified	PEN60/70	WC	19	Gabbro	4.10	5.20	14.60	64.40
11	PMB	PG76E-10	WC	19	Gabbro	4.30	6.10	15.30	60.10
12	PMB	PG76E-10	WC	19	Gabbro	4.10	6.00	14.40	58.30
13	PMB	PG76E-10	WC	19	Gabbro	4.10	5.20	14.20	63.40
14	PMB	PG76E-10	WC	19	Gabbro	4.00	5.90	14.80	60.10
15	PMB	PG76E-10	WC	19	Gabbro	4.30	6.00	15.70	61.80
16	PMB	PG76E-10	WC	19	Gabbro	4.30	5.70	15.00	62.00
17	Unmodified	PEN60/70	ABC	25	Gabbro	3.90	6.90	14.70	53.20
18	15 % RAB	PG70S-22	ABC	25	Gabbro	3.70	6.80	14.70	53.40
19	25 % RAB	PG70S-16	ABC	25	Gabbro	3.50	6.90	14.70	53.10
20	35 % RAB	PG76S-10	ABC	25	Gabbro	3.50	6.90	15.40	55.20

In order to represent the aggregate grading in all 20 mixtures in this study, minimum and maximum percent passing at each sieve seize through the whole mixtures are collected and represented in Figure 5 versus grading envelop of Qatar Construction Specification (QCS) 2014. Based on Figure 5, it is clearly noticed that all mixtures follow a well-graded aggregate composition.

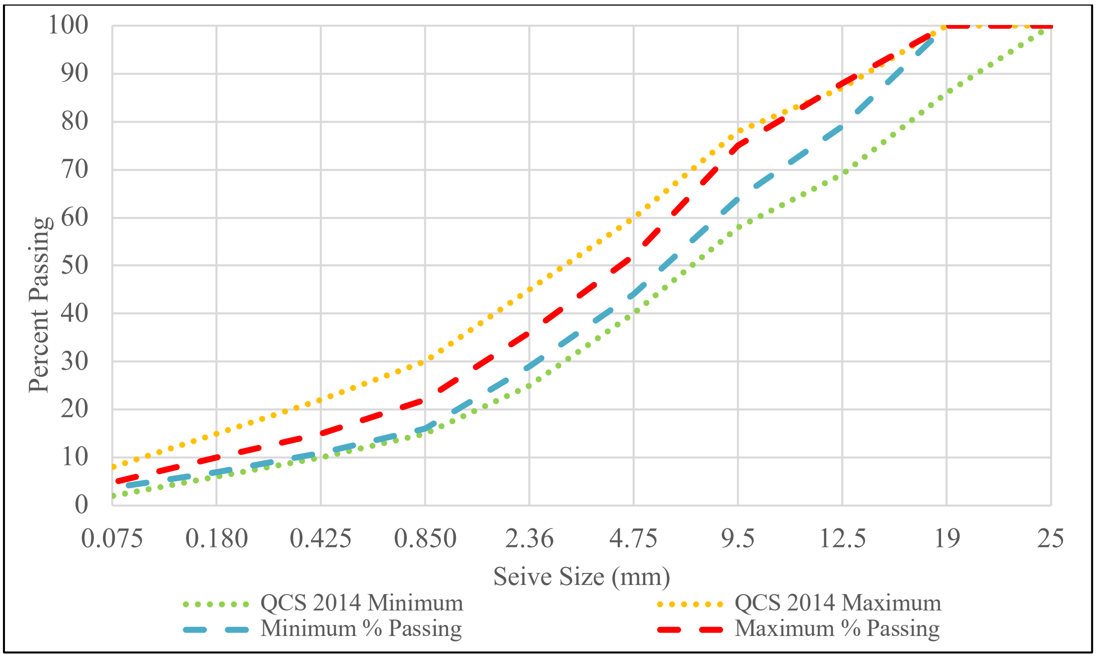

Figure 5. Aggregate Grading Envelop of QCS 2014 vs. Grading Envelop in the Study Dataset

Figure 6 below shows all PEN60/70 master curves of the collected dataset.

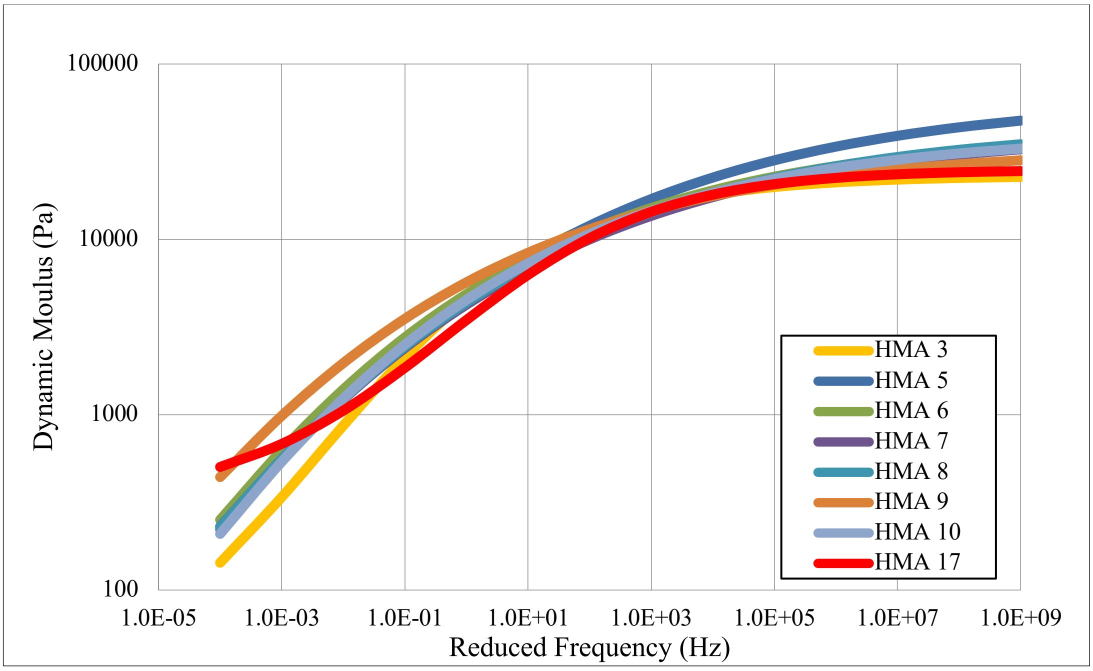

Figure 6. PEN60/70 Mixtures Master Curves of the Collected Dataset

Figure 7 below shows all PG67E-10 master curves of the collected dataset.

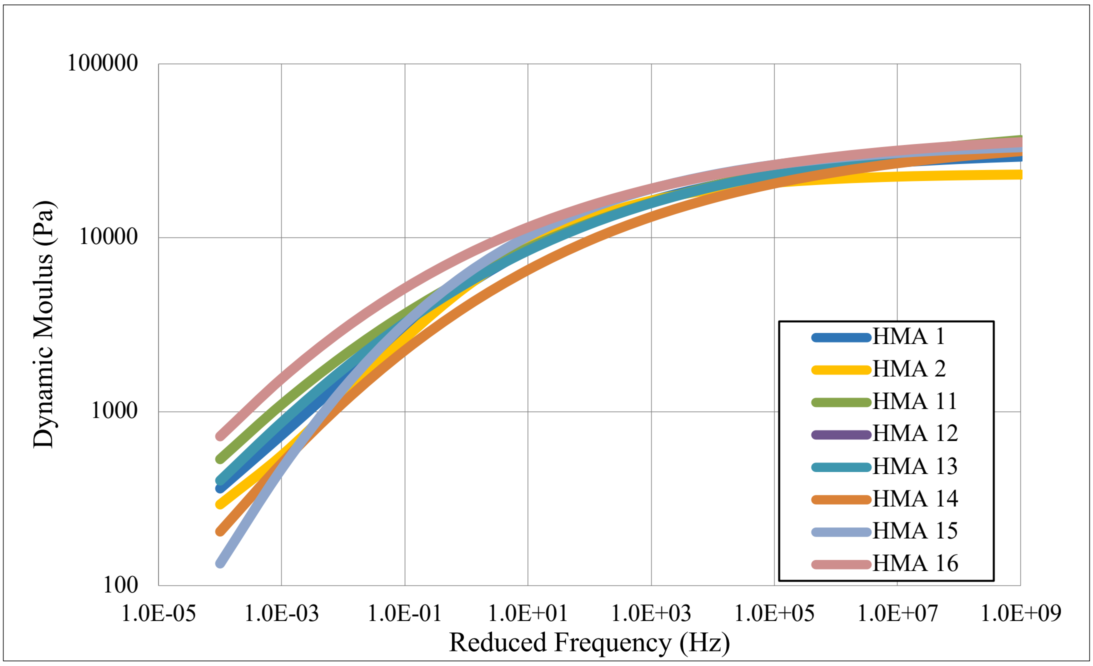

Figure 7. PG76E-10 Mixtures Master Curves of the Collected Dataset

Figure 8 below shows all PG67E-10 master curves of the collected dataset.

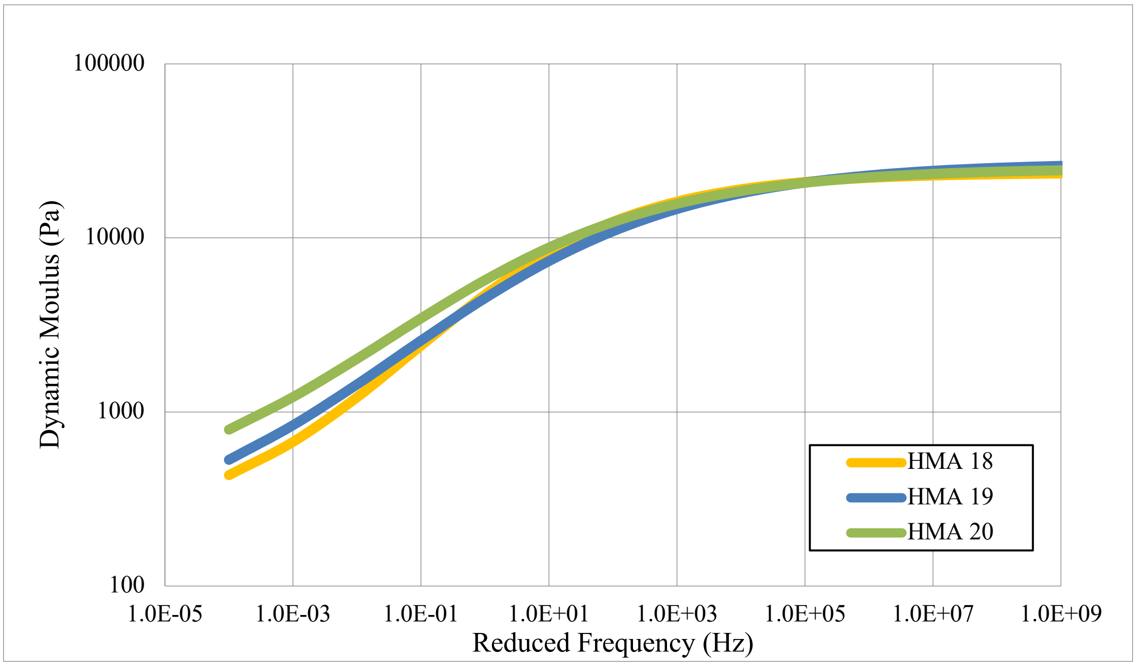

Figure 8. RAB Mixtures Master Curves of the Collected Dataset

Figure 9 below shows the only collected CRMB master curve of the collected dataset.

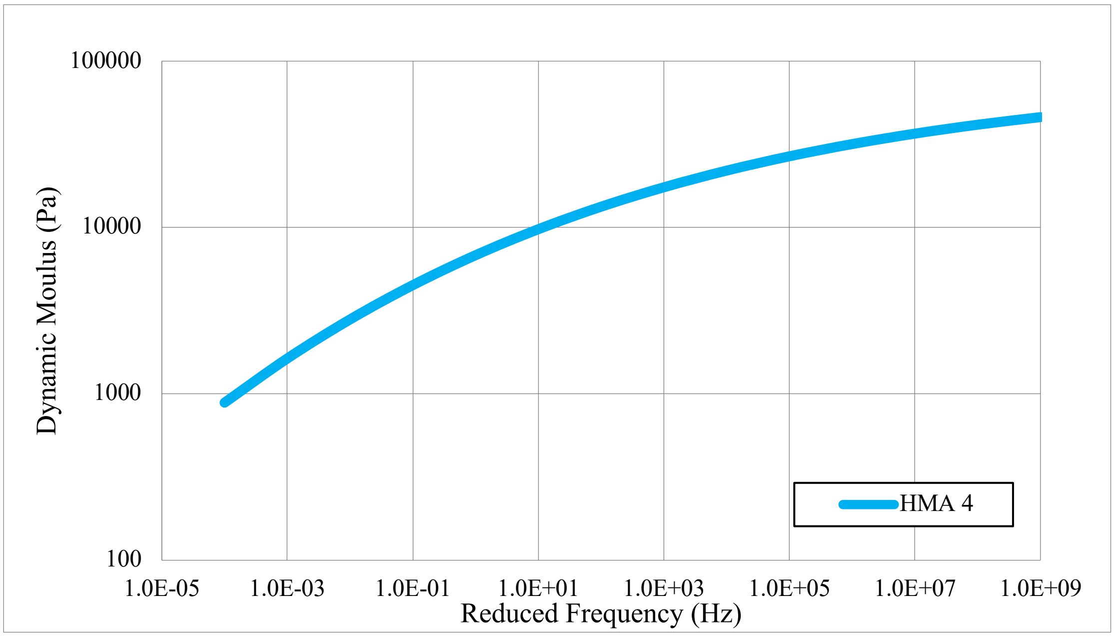

Figure 9. CRMB Mixture Master Curve of the Collected Dataset

Validation and Calibration Technique

For the validation and calibration of the Hirsch and Alkhateeb models, 393 measured dynamic moduli for 20 mixtures are used for comparison with the predicted values from the two models. A broad spectrum of frequencies and temperatures is included in the collected dataset. Table 11 shows the testing temperatures and frequencies of the collected dataset of mixtures.

Table 11. Testing Temperatures and Frequencies of Mixtures Dataset

Group No.	**HMA No.***	**Temperature (℃)**	**Frequency (Hz)**
Group 1	1, 2, 3, 4	4, 20, and 45	0.1, 1.0, and 10
Group 2	5, 6, 7, 8, 9, 10	4, 40, and 40	0.1, 0.2, 0.5, 1.0, 2.0, 5.0, 10.0, and 20.0
Group 3	11, 12, 13, 14, 15, 16	4, 20, and 45	0.1, 0.2, 0.5, 1.0, 2.0, 5.0, 10.0, and 20.0
Group 4	17, 18, 19, 20	5, 15, 25, 35, 45	0.1, 1.0, and 10.0

* HMA numbers based on Table 9 and Table 10

After comparing the Hirsch and Alkhateeb models' predicted dynamic modulus values versus the measured ones, the coefficient of determination (R^2) and S_e/S_y values were computed as goodness-of-fit measures using Equations (12), (13), and (14) (Yousefdoost et al., 2013).

$$R^2 = 1 - \frac{(n-k-1)}{(n-1)}\left(\frac{S_e}{S_y}\right)^2 \tag{12}$$

Where:

n =	Number of testing points
k =	Count of regression coefficients in the prediction model
S_e =	Standard error of estimation
S_y =	Standard deviation of the measured values

Where:

$$S_y = \sqrt{\frac{\sum_{i=1}^{n}(E_{mi}^* - \bar{E}_m^*)^2}{(n-1)}} \tag{13}$$

$$S_e = \sqrt{\frac{\sum_{i=1}^{n}(E_{pi}^* - \bar{E}_{mi}^*)^2}{(n-k-1)}} \tag{14}$$

Where:

E_{mi}^* =	Measured dynamic modulus value
$\bar{E}_m^*$ =	Average of dynamic modulus measured values
E_{pi}^* =	Dynamic modulus predicted value

In order to interpret the computed values of R^2 and S_e/S_y, the criterion in Table 12 is followed (Pellinen, Kristiina, 2001).

Table 12. Statistical Criterion for Association of Measured E^* versus predicted E^*

Criterion	**R^2 (%)**	**S_e/S_y**
Excellent	> 90	<0.35
Good	70-89	0.36-0.55
Fair	40-69	0.56-0.75
Poor	20-39	0.76-0.90
Very Poor	<19	>0.90

Statistical bias has also been used to determine both models' predictive performance by finding the slope and intercept of the linear trend line of the measured vs. predicted plot. The higher prediction performance would be subjected to a slope closer to one and an intercept closer to zero (Solatifar, 2020).

To calibrate the models, the excel solver is utilized to minimize the error and maximize the fit by reducing the Route Mean Square Error (RMSE) that computed using formula shown in equation (15) (Cano-Ortiz et al., 2022).

$$RMSE = \sqrt{\frac{\sum_{i=1}^{n}(E_{mi}^{*} - E_{pi}^{*})^{2}}{n}} \tag{15}$$

Where:

RMSE = Root Mean Square Error

Based on the error minimization results, new fitting parameters for the Hirsch model (i.e., h_1, h_2, and h_3) are found instead of 20, 650, and 0.58, respectively, in Equation (5). The same approach is followed for the Alkhateeb model to find k_1 - k_6 coefficients instead of 3, 90, 1.45, 0.66, 1100, and 0.13, respectively, in Equation (8).

Methodology Summary

The following steps represent the methodology summary that is explained in above sections:

1- Substitute the volumetrics (VMA/VFA) and G^* in both Hirsch (Equation (4) and Alkhateeb (Equation (5) models and find E^* using excel.

2- Calculate RMSE using Equation (15) after comparing predicted vs. measured E^*.

3- Use solver in excel in order to minimize the RMSE by changing the empirical fitting parameters of each model that is determined in the previous chapter.

4- Define the new fitting parameters after conducting the error minimization.

5- Calculate the R^2, Se/Sy, Slope, and Intercept for each scenario.

CHAPTER 4: RESULTS AND DISCUSSION

Introduction

In this chapter, the validation and calibration results and the statistical findings are presented, discussed, and compared to the reviewed literature. The chapter also includes the aforementioned sensitivity study conducted on the Hirsch and Alkhateeb models. The chapter's conclusion displays the findings of functional performance analysis done on Qatari pavement sections before and after calibration to emphasize the significance of the calibration.

Validation and Calibration

The R^2 value of prediction performance for the Hirsch model before and after calibration is 87.2% and 89.2%, respectively. Figure 10 and 11 show measured versus predicted E^* before and after calibration of the Hirsch model, respectively. The R^2 value of prediction performance for the Alkhateeb model before and after calibration is 70.8% and 89.2%, respectively. Figure 12 and 13 show measured versus predicted E^* before and after calibration of the Alkhateeb model, respectively.

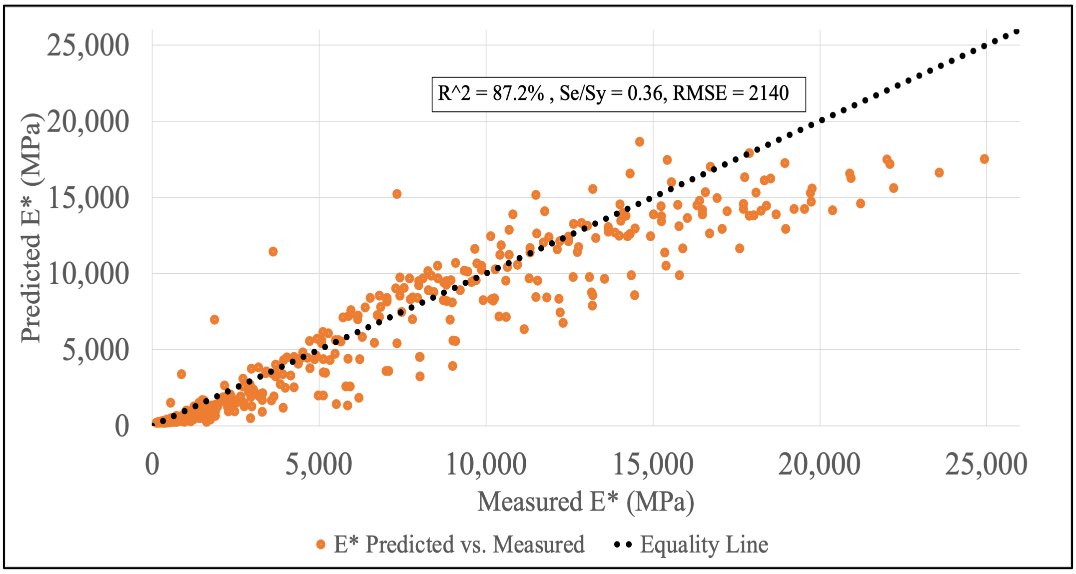

Figure 10. Predicted vs. Measured E^* before Calibration – Hirsch Model

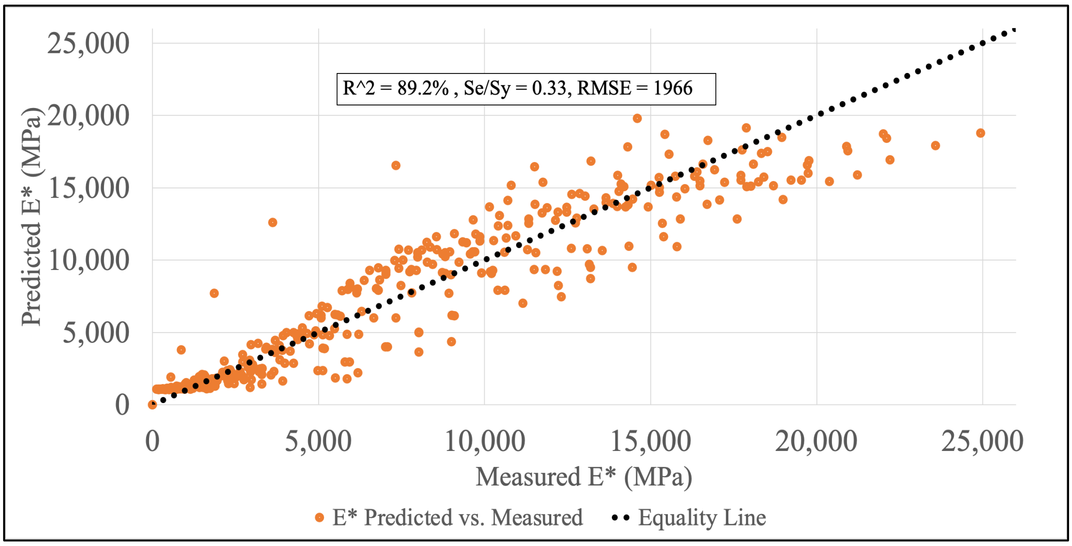

Figure 11. Predicted vs. Measured E^* After Calibration – Hirsch Model

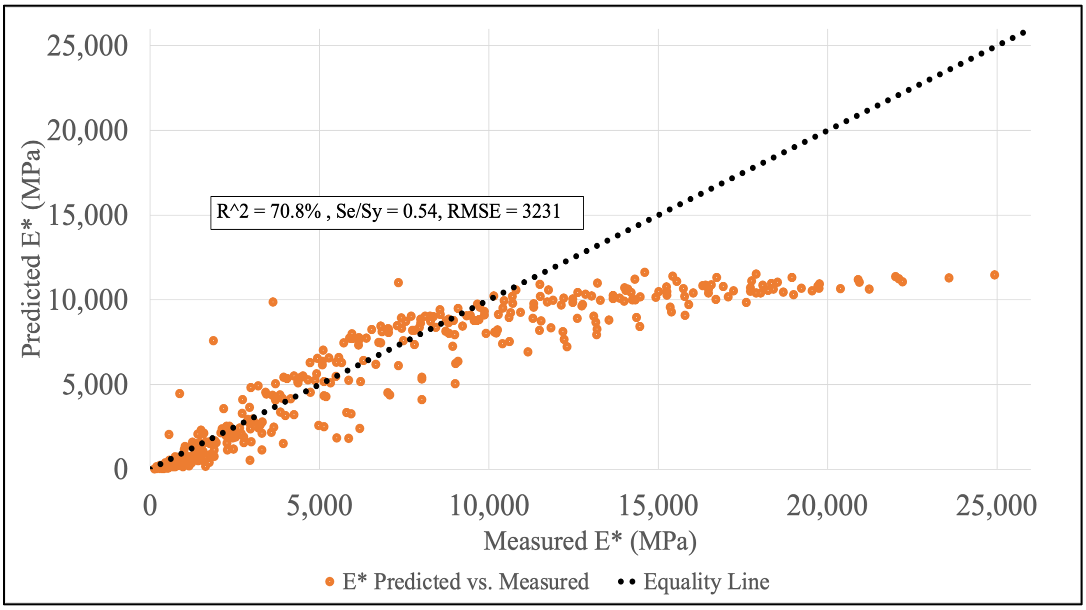

Figure 12. Predicted vs. Measured E* before Calibration – Alkhateeb Model

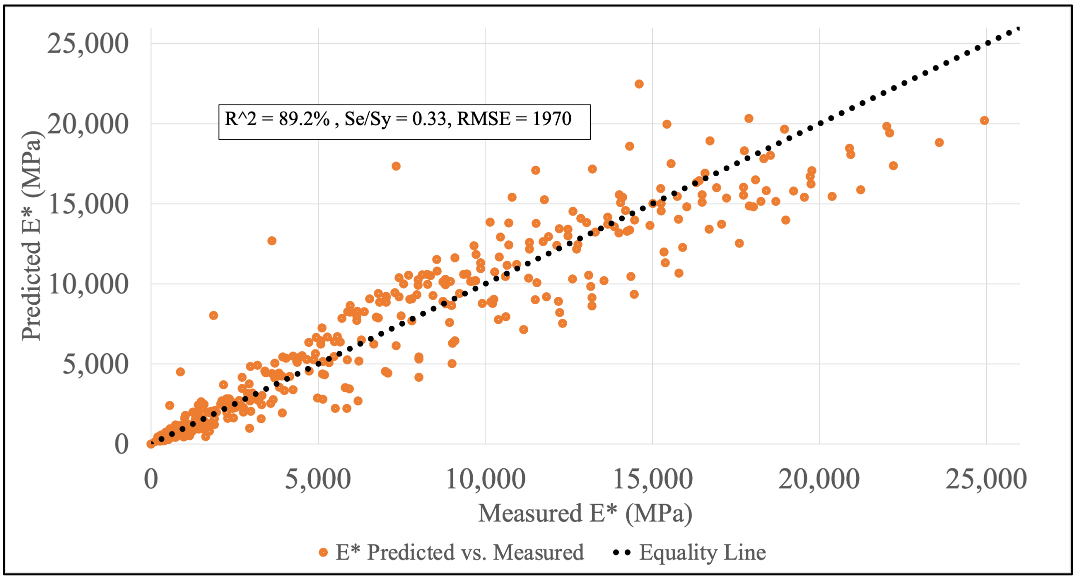

Figure 13. Predicted vs. Measured E* after Calibration – Alkhateeb Model

Table 13 shows the goodness-of-fit measures and their correlation for both Hirsch and Alkhateeb models before and after calibration.

Table 13. Hirsch and Alkhateeb Overall Models Goodness-of-fit Values

Model	Before Calibration				After Calibration			
	R^2	Correlation	Se/Sy	Correlation	R^2	Correlation	Se/Sy	Correlation
Hirsch	87.2%	Good	0.36	Good	89.2%	Good	0.33	Excellent
Alkhateeb	70.8%	Good	0.54	Good	89.2%	Good	0.33	Excellent

Table 14 shows bias measures for both Hirsch and Alkhateeb models before and after calibration.

Table 14. Hirsch and Alkhateeb Overall Models Bias Measures

Model	Before Calibration		After Calibration	
	Slope	Intercept	Slope	Intercept
Hirsch	0.848	214.37	0.900	716.98
Alkhateeb	0.612	1116.10	0.900	652.75

As presented in Table 13 and 14, the Hirsch model shows high prediction performance without calibration with an R^2 value of 87.2% and a slope of 0.848. After calibration, the R^2 value improved slightly to 89.2%, and the slope improved to 0.900. This improvement of 2.0% in R^2 value is close to the study of Robbins and Timm outcomes (Robbins & Timm, 2011) for the southeastern United States asphalt mixtures that used a similar error minimization approach to improve the Hirsch model R^2 value from 89.7% to 91.1%.

Alkhateeb model shows reasonable prediction performance prior to calibration over a wide variety of frequencies and temperatures. However, the findings show that the model underpredicts the E^* through a significant number of testing points with exponential trends resulting in a low R^2 value of 70.8% and a high bias at the slope of 0.612. The calibration of the model improved the R^2 value to become 89.2%.

The predictive performance of both the Hirsch and Alkhateeb models comes in contrary to Yousefdoost et al. (Yousefdoost et al., 2013) study, which concluded that none of the Hirsch and Alkhateeb models are suitable for use for Australian asphalt mixtures developed for a hot climate country.

It to be note that both models after calibration showed almost same goodness-of-fit and bias and this would be due to that both models derived from the rule of mixture and has quiet similar derivation, inputs, and assumptions.

Sensitivity Analysis

Sensitivity analysis was conducted for the calibrated Hirsch and Alkhateeb models to investigate the sources of prediction errors and relate the results to the local Qatar conditions. R^2 and S_e/S_y were calculated for the prediction performance for both Hirsch and Alkhateeb models by varying one factor of binder type, temperature, or frequency at a time while keeping the other factors constants. Table 15 and 16 present the R^2 values of the Hirsch and Alkhateeb models for several binder types, respectively. Table 17 and 18 show the R^2 of the Hirsch and Alkhateeb models for several testing temperatures, respectively.

Table 19 and 20 present the R^2 of the calibrated Hirsch and Alkhateeb models for several frequencies, respectively.

Table 15. Binder Sensitive Predictive Performance of the Hirsch Model

Binder Type			**PEN 60/70**		**PG 76E-10**		**RAB (15, 25, 35)%**	
No. of Data Points			**169**		**164**		**45**	
Calibration	**Before**	**R^2**	94.40%	Excellent	86.40%	Good	63.10%	Fair
		Se/Sy	0.24	Excellent	0.37	Good	0.63	Fair
	After	**R^2**	94.60%	Excellent	90.50%	Excellent	50.90%	Fair
		Se/Sy	0.23	Excellent	0.31	Excellent	0.73	Fair

Table 16. Binder Sensitive Predictive Performance of the Alkhateeb Model

Binder Type			PEN 60/70		PG 76E-10		RAB (15, 25, 35)%	
No. of Data Points			**169**		**164**		**45**	
Calibration	**Before**	**R^2**	78.6%	Good	65.9%	Fair	70.8%	Good
		Se/Sy	0.47	Good	0.59	Fair	0.58	Fair
	After	**R^2**	95.1%	Excellent	91.1%	Excellent	41.2%	Fair
		Se/Sy	0.23	Excellent	0.30	Excellent	0.83	Poor

Table 17. Temperature Sensitive Predictive Performance of the Hirsch Model

Temperature			4 and 5 °C		15, 20 and 25 °C		35, 40 and 45 °C	
No. of Data Points			**122**		**134**		**137**	
Calibration	**Before**	**R^2**	35.6%	Poor	42.8%	Fair	17.5%	Very Poor
		Se/Sy	0.81	Poor	0.77	Poor	0.92	Very Poor
	After	**R^2**	51.0%	Fair	40.6%	Fair	36.9%	Poor
		Se/Sy	0.71	Fair	0.78	Poor	0.80	Poor

Table 18. Temperature Sensitive Predictive Performance of the Alkhateeb Model

Temperature			4 and 5 °C		15, 20 and 25 °C		35, 40 and 45 °C	
No. of Data Points			**122**		**134**		**137**	
Calibration	**Before**	**R^2**	-94.8%	Very Poor	53.9%	Fair	15.0%	Very Poor
		Se/Sy	1.41	Very Poor	0.69	Fair	0.93	Very Poor
	After	**R^2**	48.6%	Fair	44.4%	Fair	38.4%	Poor
		Se/Sy	0.73	Fair	0.75	Fair	0.79	Poor

Table 19. Frequency Sensitive Predictive Performance of the Hirsch Model

Frequency (Hz)	n*	Before Calibration				After Calibration			
		R^2		Se/Sy		R^2		Se/Sy	
0.1	68	78.30%	Good	0.48	Good	81.90%	Good	0.44	Good
0.2	39	81.70%	Good	0.45	Good	84.90%	Good	0.40	Good
0.5	36	88.50%	Good	0.36	Good	90.70%	Excellent	0.32	Excellent
1	68	89.00%	Good	0.34	Excellent	89.90%	Good	0.32	Excellent
2	36	90.00%	Excellent	0.33	Excellent	92.80%	Excellent	0.28	Excellent
5	36	89.40%	Good	0.34	Excellent	92.50%	Excellent	0.29	Excellent
10	68	83.40%	Good	0.42	Good	83.70%	Good	0.41	Good
20	39	84.60%	Good	0.41	Good	88.90%	Good	0.35	Excellent

* n = Number of data points

Table 20. Frequency Sensitive Predictive Performance of the Alkhateeb Model

Frequency (Hz)	n*	Before Calibration				After Calibration			
		R^2		Se/Sy		R^2		Se/Sy	
0.1	68	80.60%	Good	0.46	Good	83.80%	Good	0.42	Good
0.2	39	80.40%	Good	0.48	Good	86.50%	Good	0.40	Good
0.5	36	80.60%	Good	0.48	Good	91.20%	Excellent	0.33	Excellent
1	68	78.70%	Good	0.48	Good	89.00%	Good	0.35	Excellent
2	36	71.50%	Good	0.59	Fair	92.60%	Excellent	0.30	Excellent
5	36	63.70%	Fair	0.66	Fair	92.60%	Excellent	0.30	Excellent
10	68	59.70%	Fair	0.67	Fair	81.70%	Good	0.45	Good
20	39	47.30%	Fair	0.79	Poor	90.20%	Excellent	0.34	Excellent

* n = Number of data points

Figure 14 below shows the HMA 9 measured master curve versus the predicted uncalibrated and calibrated master curves as a sample of binder PEN60/70 mixtures.

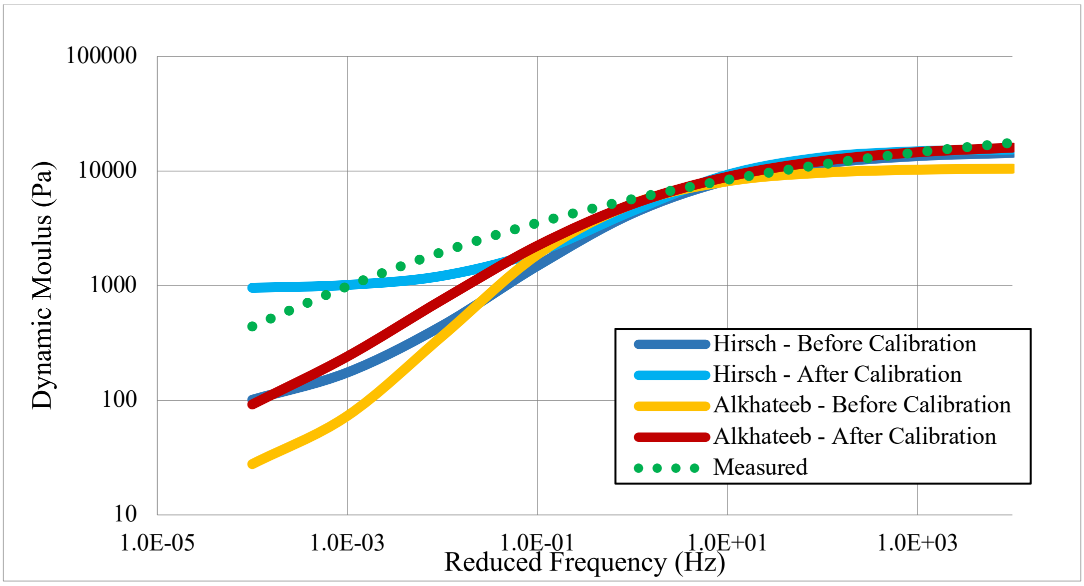

Figure 14. HMA 9 Measured and Predicted Uncalibrated and Calibrated Hirsch and Alkhateeb Models Master Curves

Figure 15 below shows the HMA 9 measured master curve versus the predicted uncalibrated and calibrated master curves as a sample of binder PG76E-10 mixtures.

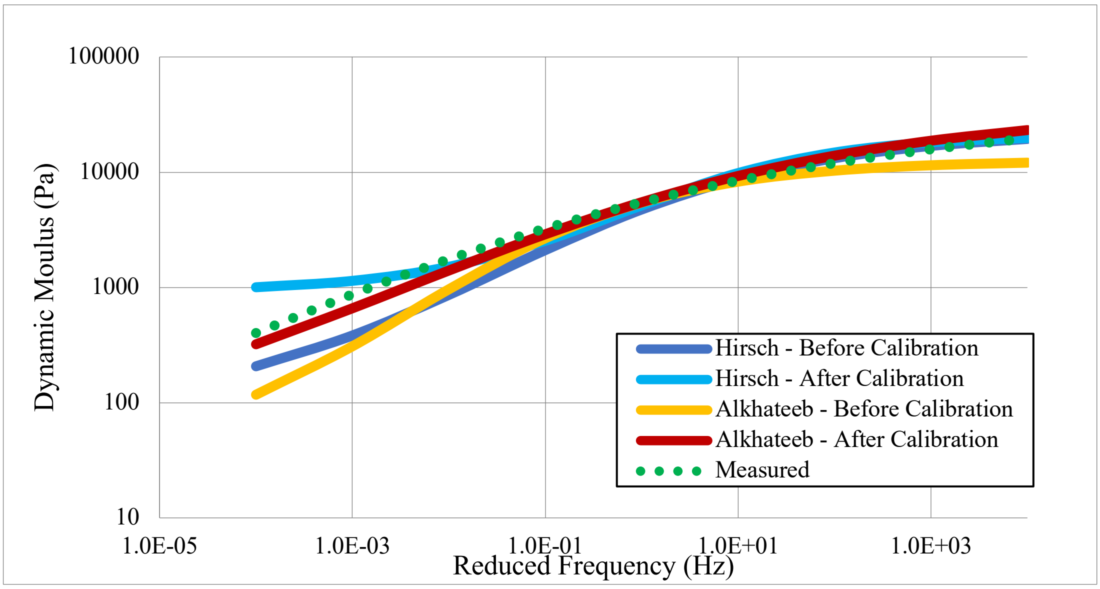

Figure 15. HMA 13 Measured and Predicted Uncalibrated and Calibrated Hirsch and Alkhateeb Models Master Curves

Figure 16 below shows the HMA 20 measured master curve versus the predicted uncalibrated and calibrated master curves as a sample of RAB mixtures.

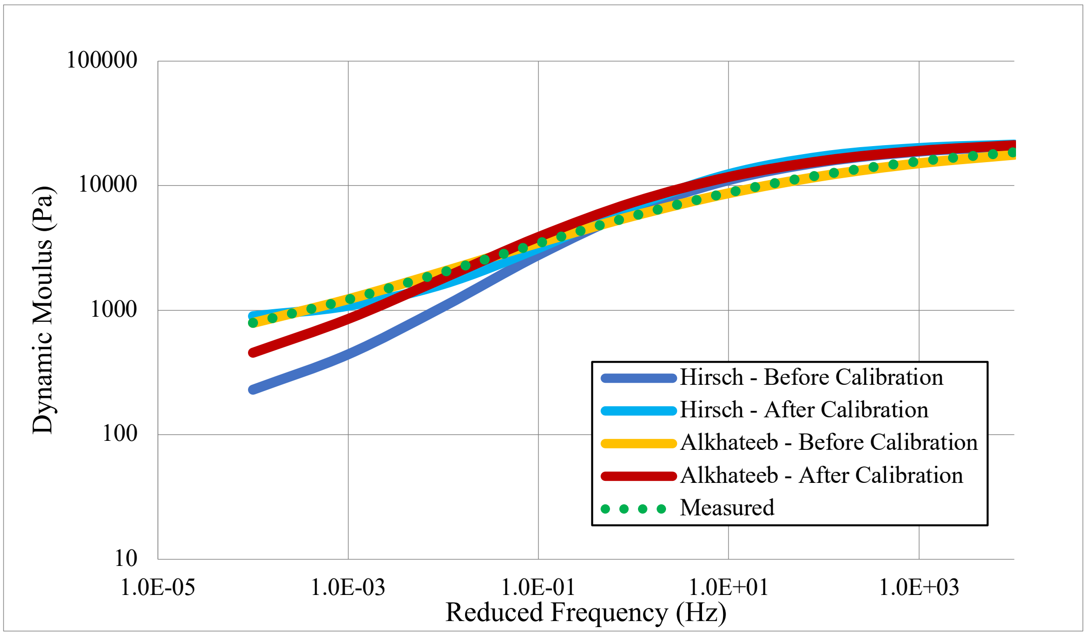

Figure 16. HMA 20 Measured and Predicted Uncalibrated and Calibrated Hirsch and Alkhateeb Models Master Curves

Figure 17 below shows the HMA 4 measured master curve versus the predicted uncalibrated and calibrated master curves as a sample of CRMB mixture.

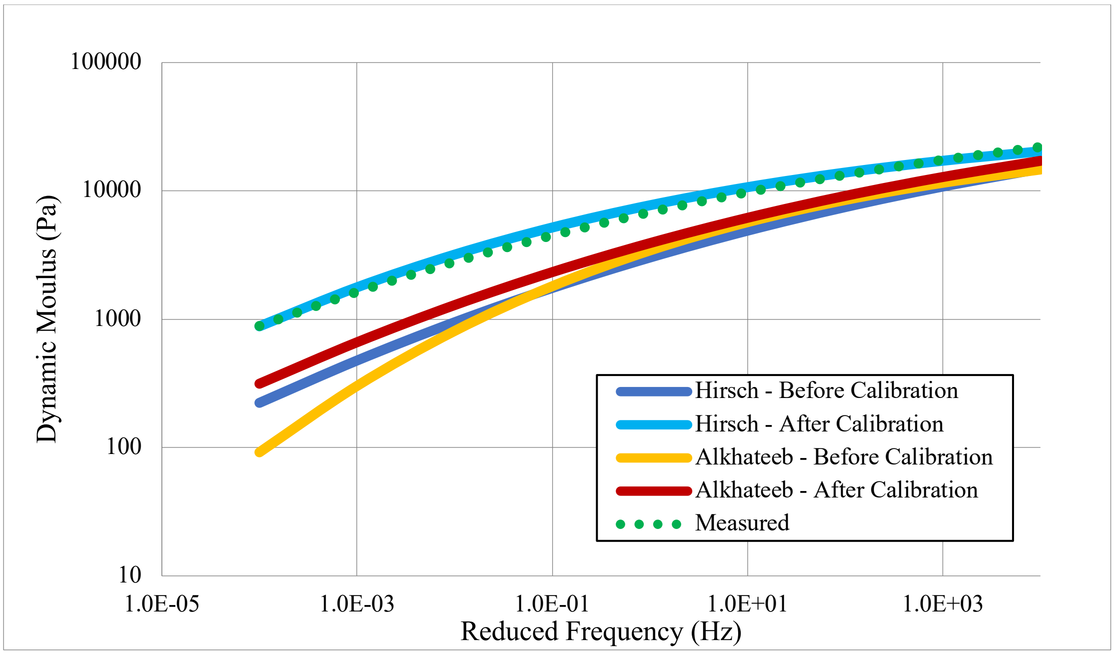

Figure 17. HMA 4 Measured and Predicted Uncalibrated and Calibrated Hirsch and Alkhateeb Models Master Curves

Sensitivity analysis results conclude that the calibrated Alkhateeb model shows equivalent performance to the calibrated Hirsch model for all types of binder mixtures. However, uncalibrated models offer superior performance to the Hirsch model in a PEN60/70 and PG 76E-10 but lower performance in RAB mixtures. This can be because the Alkhateeb model was developed based on a dataset of aged materials (Al-Khateeb et al., 2006). It is noticed that the calibration reduced the prediction performance of both models for RAB mixtures.

For testing frequency sensitivity, the uncalibrated Hirsch model shows superior performance over the Alkhateeb model, as the last has a significantly increasing bias toward higher frequencies. After calibration, the Alkhateeb model bias at high frequency is reduced significantly.

For temperature sensitivity, both uncalibrated models show very poor predictive performance at high testing temperatures of 35 – 45 °C, which has been improved after calibration, which agrees with (Far et al., 2009) study that showed a noticeable bias of the Hirsch model at high temperatures. Looking at Figure 12, Tables 18 and 20, it can be inferred that the uncalibrated Alkhateeb model has poor prediction at testing temperatures 4 – 5 ℃ and 10 – 20 Hz testing frequency which is improved after calibration, as shown in Figure 13. This result agrees with the outcomes of (Yousefdoost et al., 2013) which was conducted on Australian Asphalt mixtures, and (Far et al., 2009) study, which was conducted on a comprehensive dataset of Witzack, Federal Highway Administration (FHWA), and others. The Hirsch model performance at low temperature was higher than the Alkhateeb model, which agrees with (Far et al., 2009) study outcome. However, the low predictability at such low temperatures is not a concern in Qatar because these temperatures are rare, as shown in Figure 1. Table 21 and 22 show the fitting parameters for Hirsch and Alkhateeb models, respectively.

Table 21. Fitting Parameters for the Hirsch Model (Equation (4)

Fitting Factor	**Before Calibration**	**After Calibration**
h_1	20	348
h_2	650	897
h_3	0.58	0.63

Table 22. Fitting Parameters for the Alkhateeb Model (Equation (8)

Fitting Factor	**Before Calibration**	**After Calibration**
k_1	3.00	6.76
k_2	90.00	92.69
k_3	1.45	2.67
k_4	0.66	0.42
k_5	1100.00	255.69
k_6	0.13	0.01

Pavement Performance Analysis

This section compares the functional distresses of pavement profiles typically used in Qatar, considering the modulus of the Hirsch model before and after calibration. This was accomplished by evaluating the rutting and fatigue cracking performance using the Mechanistic-Empirical Asphalt Pavement Analysis (MEAPA) web application developed by (Kutay & Lanotte, 2020). This web-based application considers the same traffic inputs of the MEPDG (NCHRP, 2004). The MEAPA climatological inputs are equivalent to the MEPDG Enhanced Integrated Climatic Model (EICM). Equation (9) presented earlier in this report is considered in the MEAPA application to interpret the master curve. Calculations of the loading frequency are based on the concepts used by the MEPDG, where the stress pulse is assumed to be haversine, and its duration relies on the vehicle's speed and the depth from the wearing course top to the point of interest. In addition, the basic propagation of the thermal crack length within the depth of the pavement is found based on a simplified Paris law. MEAPA application has several climatological profiles covering several areas and climates worldwide that can be chosen as preliminary analysis to have a more accurate site-specific simulation.

Three pavement structures for different road hierarchies and traffic loading conditions are employed in the analysis to simulate the actual pavement structures used in Qatar.

Figure 18 shows pavement structures for the collected three pavement sections for different road reliabilities of 75%, 90%, and 97% corresponding to local, arterial, and expressway road hierarchies, respectively, based on Qatar Highway Design Manual (QHDM) (MOTC, 2015). The selected three pavement structures have three different traffic loading levels indicated as Equivalent Single Axle Loads (ESALs).

Figure 19 shows a binder-type matrix for the collected pavement structures for the asphalt Wearing Course (WC), Asphalt Intermediate Course (AIC), and Asphalt Base Course (ABC) layers.

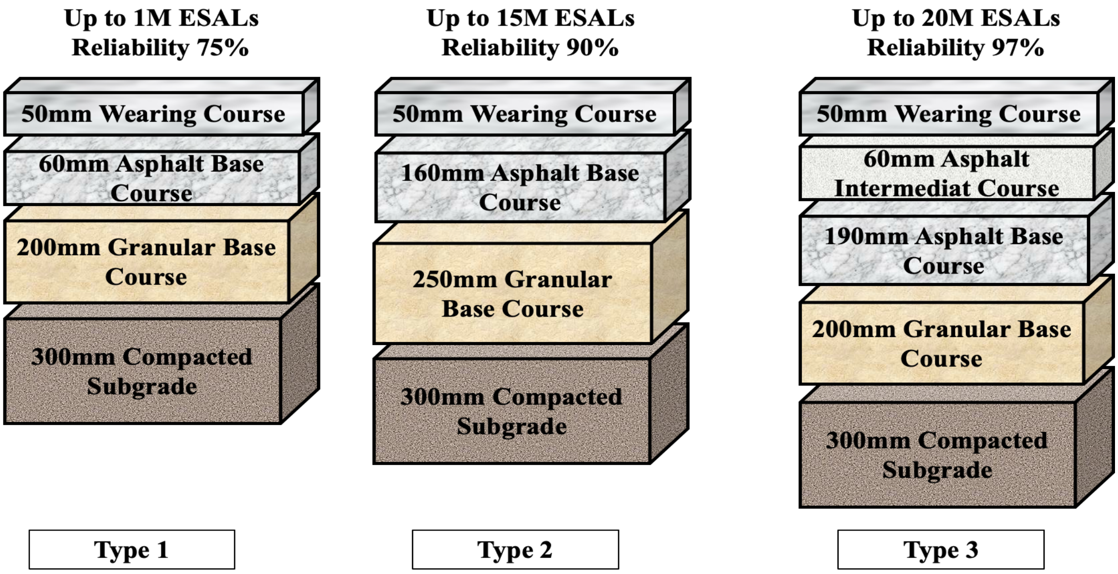

Figure 18. Illustration of Three Pavement Structures

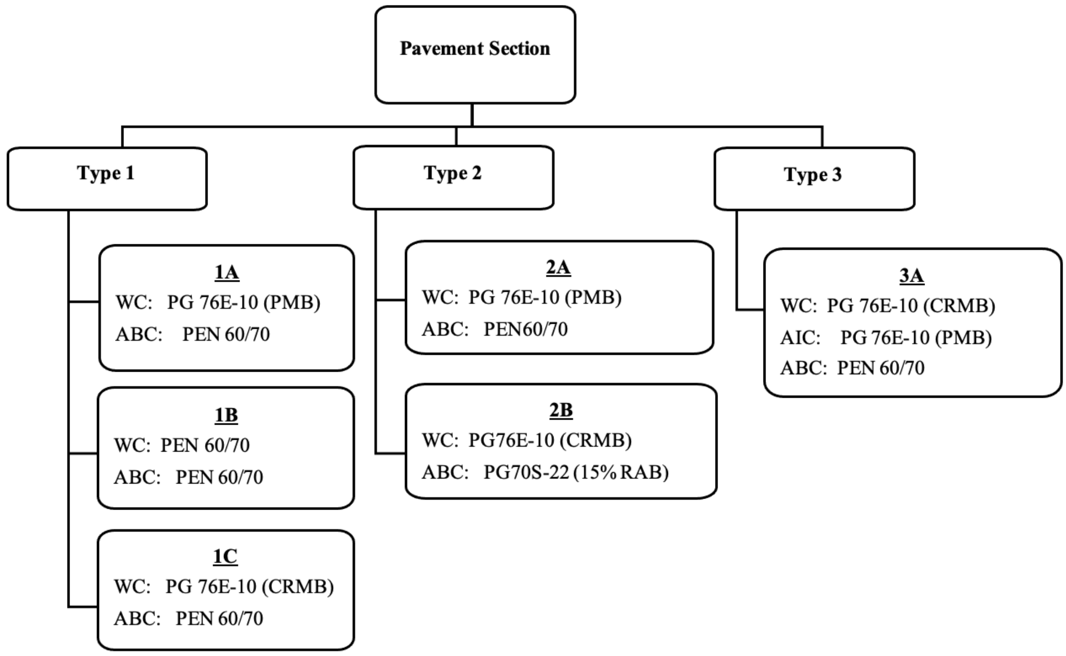

Figure 19. Binder Type Matrix for the Collected Pavement Structures

In the MEAPA web application, the nearest available climatological profile to the State of Qatar was for Dammam city, located in the eastern area of Saudi Arabia. Dammam city is a 180 km air distance from Doha city, the capital of Qatar. In order to validate the Dammam city climatological profile to represent Qatar, monthly mean temperatures data for Dammam was collected from the Saudi National Center for Meteorology (NCM) website (NCM, n.d.) and compared with the data collected from the Qatar Meteorology Department website (QMD, n.d.-a). Figure 20 shows the mean monthly temperature normals for Doha and Dammam cities. As shown in Figure 20, Doha and Dammam have similar mean temperature climatological normals with only minor differences. Accordingly, Dammam's climatological profile is considered valid to represent Qatar's climate. Table 23 shows the traffic inputs used in the ME analysis on the MEAPA website.

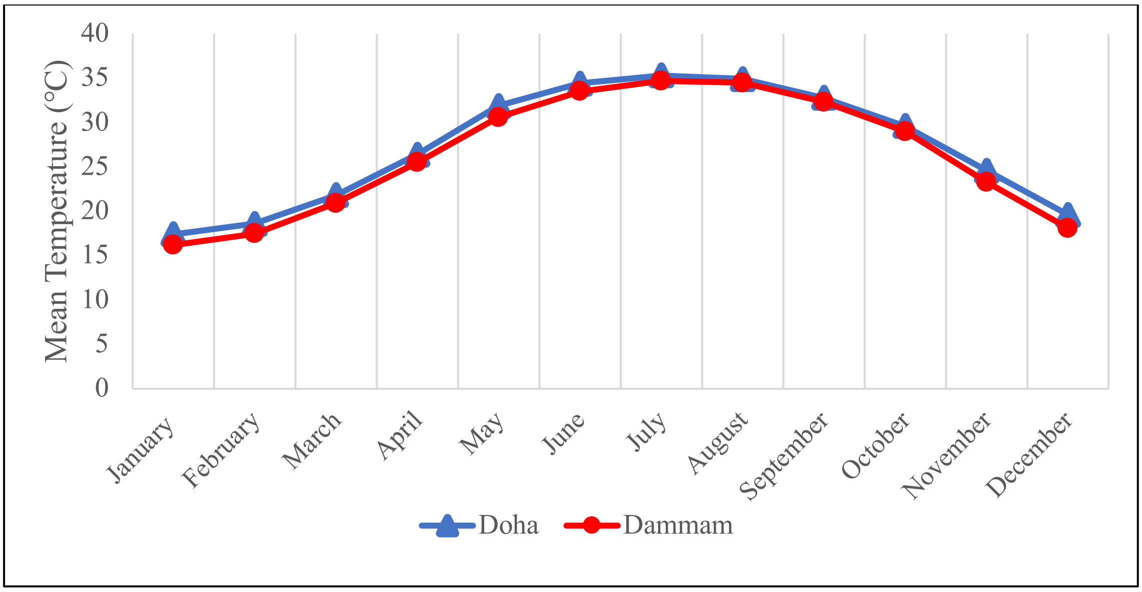

Figure 20. Mean monthly temperatures for Doha and Dammam cities

Table 23. Traffic Load Inputs for ME Analysis on the MEAPA Website

Traffic Parameter	Pavement Structure*		
	Type 1	**Type 2**	**Type 3**
AADT** (veh/day)	220	3344	6672
Lane Factor	1.00	0.90	0.60
Distribution Factor	0.55	0.55	0.55
Speed (kph)	50	60	100
Analysis Period (yrs)	20	20	20

* Refer to Figure 18 and Figure 19 for pavement structures and binder types
** AADT stands for Annual Average Daily Traffic

It is to be noted that the vehicle fleet profile, monthly distribution, and other related entries were kept as default in the MEAPA software. Table 24 shows the performance results and percent change before and after calibration for pavement structures Type 1, 2, and 3. Detailed analysis results are attached to Appendix A.

Table 24. Change in the Fatigue and Rutting due to Hirsch model Calibration

Pavement Section*	**Fatigue (m/km)**		**Percent**	**Rutting (cm)**		**Percent**
Calibration Status	**Before**	**After**	**Change**	**Before**	**After**	**Change**
1A	126.06	157.50	24.94%	0.51	0.58	13.73%
1B	143.47	224.51	56.49%	0.51	0.53	3.92%
1C	188.31	180.30	-4.25%	0.53	0.53	0.00%
2A	662.23	892.19	34.73%	0.71	0.79	11.27%
2B	870.40	746.44	-14.24%	0.71	0.66	-7.04%
3A	578.69	615.22	6.31%	0.64	0.64	0.00%
Average =			**17.33%**			**3.65%**

* Refer to Figure 18 and Figure 19 for pavement structures and binder types

As shown in Table 24, the difference in the predicted distress, whether a decrease or increase due to calibration, is more significant in the fatigue life predictions than the rutting predictions. For the case of fatigue life, the difference due to local calibrations reached more than 50%, with an average value of 17.33%. This result agrees with (Cooper et al., 2015) study, which concluded that the predicted alligator cracking would change by 60% with changing the dynamic modulus value. In addition, this result agrees with (Cheng et al., 2021) study, which concluded that changing the E^* value in the MEPDG analysis procedure would significantly change the predicted field strains. Accordingly, using locally calibrated is required to give more reliable pavement performance prediction and designs.

Despite that R^2 of the Hirsch model prediction performance was improved by around 2%, which is considered insignificant in another study (Robbins & Timm, 2011), the new dynamic modulus values have changed the predicted distresses of pavement structures. This implements the importance of investigating the practical effect of calibration in this field.

CHAPTER 5: CONCLUSIONS AND RECOMMENDATIONS

Conclusions

The study reviewed the Hirsch, Witzack 1-37A, Witzack 1-40D, and Alkhateeb models and evaluated and calibrated the Hirsch and Alkhateeb models based on local Qatari materials representing countries with hot and humid climates. The research study considered the empirical calibration method and highlighted the sensitivity of the models' calibration on the predicted functional pavement performance by conducting the MEAPA method analysis on pavement structures before and after calibration. The results of the investigation mentioned above lead to the following conclusions:

- Hirsch model showed high prediction performance for Qatar asphalt mixtures with an R^2 value of 87.2% prior to calibration. Alkhateeb model, however, showed lower performance with an R^2 value of 70.8%. The calibration improved the R^2 value of the Hirsch and Alkhateeb models to 89.2% for both.
- The sensitivity analysis showed that the Hirsch and Alkhateeb models had higher performance in PEN 60/70 and PG 76E-10 mixtures and lower performance in RAB mixtures.
- While the implemented calibration technique improved the overall performance of both models, more bias was introduced for RAB mixtures in both models after calibration.
- Both uncalibrated Hirsch and Alkhateeb models had a low predictive performance at test temperatures higher than 35°C, which improved with model calibration.
- Hirsch model showed consistent performance over-tested frequencies between 0.1 and 20 Hz with an R^2 value ranging between 70 and 90%. However, the uncalibrated Alkhateeb model showed significant bias at high frequencies.

- The uncalibrated Alkhateeb model showed poor performance at low temperatures of 4 – 5°C and a frequency of 10 – 20 Hz. This performance was improved as a result of the model calibration.
- Mechanistic-Empirical analysis for pavement structures of Qatar showed significant change in the predicated fatigue distress, reaching more than 50% after considering the calibrated master curve of the asphalt mixtures with an average value of 17.33%. This result confirmed that using the locally calibrated models will give more reliable pavement performance prediction and designs.
- While the calibration changed the R^2 value of the Hirsch model only by 2%, there is a considerable variation in the predicted pavement performance using the MEAPA method. This result emphasizes the consideration of the practical effect of the calibration in this field.

Recommendations

Through this study, several challenges were determined that should be considered in the future as follows:

- It is recommended to use the calibrated Hirsch or Alkhateeb model in Qatar instead of the uncalibrated version of the models.
- Dynamic modulus testing practice in hot climate countries such as Qatar should consider testing temperatures higher than 45°C to simulate the hot climatic conditions.
- The public work authority should develop an organized database for all projects in the country, which will open doors for further calibration and value engineering studies in the region.
- It is recommended to introduce Artificial Neural Network (ANN) and Machine Learning techniques in developing dynamic modulus prediction models after

collecting an extensive database from hot climate countries in the region.

- It is recommended to test the sensitivity of performed calibrations of prediction models on the predicted functional performance regardless of the improvement in the R^2. Accordingly, the researcher would classify the significance of the calibration technique.

References

AASHTO. (1993). AASHTO Guide for Design of Pavement Structures, 1993. The Association.

AASHTO. (2017). Standard Practice for Developing Dynamic Modulus Master Curves for Asphalt Mixtures using the Asphalt Mixture Performance Tester (AMPT). In The Association.

Abu Abdo, A. M. (2012). Sensitivity analysis of a new dynamic modulus (| E*|) model for asphalt mixtures. Road Materials and Pavement Design, 13(3), 549–555. https://doi.org/10.1080/14680629.2012.710003

Al-Khateeb, G., Shenoy, A., Gibson, N., & Harman, T. (2006). A new simplistic model for dynamic modulus predictions of asphalt paving mixtures . 2006 Annual Meeting of Association of Asphalt Paving Technologists, January.

Andrei, D., Witczak, M., & Mirza, M. (1999). Development of a Revised Predictive Model for the Dynamic (Complex) Modulus of Asphalt Mixtures. NCHRP.

Apeagyei, A. K. (2011). Rutting as a Function of Dynamic Modulus and Gradation. Journal of Materials in Civil Engineering, 23(9), 1302–1310. https://doi.org/10.1061/(asce)mt.1943-5533.0000309

Bari, J., & Witczak, M. (2006). Development of a new revised version of the Witczak E_ predictive model for hot mix asphalt mixtures (with discussion). Associated Asphalt Paving Technologies, 75, 381–423.

Bari, Javed, Witczak, M. W., You, Z., Solamanian, M., Huang, B., Mohseni, A., Dukatz, E., Chehab, G., Williams, C., & Christiansen, D. (2006). Development of a new revised version of the Witczak E Predictive Model for hot mix asphalt mixtures. Asphalt Paving Technology: Association of Asphalt Paving Technologists-Proceedings of the Technical Sessions, 75(January 2006), 381–

424.

Cano-Ortiz, S., Pascual-Muñoz, P., & Castro-Fresno, D. (2022). Machine learning algorithms for monitoring pavement performance. Automation in Construction, 139(May), 104309. https://doi.org/10.1016/j.autcon.2022.104309

Ceylan, H., Gopalakrishnan, K., & Kim, S. (2009). Looking to the future: The next-generation hot mix asphalt dynamic modulus prediction models. International Journal of Pavement Engineering, 10(5), 341–352. https://doi.org/10.1080/10298430802342690

Ceylan, H., & Kim, S. (2007). Hot Mix Asphalt Dynamic Modulus Prediction Models Using Neural Networks Approach.

Ceylan, H., Schwartz, C. W., Kim, S., & Gopalakrishnan, K. (2009). Accuracy of Predictive Models for Dynamic Modulus of Hot-Mix Asphalt. Journal of Materials in Civil Engineering, 21(6), 286–293. https://doi.org/10.1061/(asce)0899-1561(2009)21:6(286)

Cheng, H., Wang, Y., Liu, L., & Sun, L. (2021). Effects of using different dynamic moduli on predicted asphalt pavement responses in mechanistic pavement design. Road Materials and Pavement Design, May. https://doi.org/10.1080/14680629.2021.1924842

Christensen, D. W., Jr., Pellinen, T., & Bonaquist, amon F. (2003). Hirsch Model for Estimating the Modulus of Asphalt Concrete. Asphalt Paving Technologies, 72, 97–121.

Cooper, S. B., Mohammad, L. N., Elseifi, M. A., & Raghavendra, A. (2015). Dynamic modulus of asphalt mixtures: Evaluation of effects on pavement performance prediction. Transportation Research Record, 2507, 67–77. https://doi.org/10.3141/2507-08

El-Badawy, S., Abd El-Hakim, R., & Awed, A. (2018). Comparing Artificial Neural Networks with Regression Models for Hot-Mix Asphalt Dynamic Modulus Prediction. Journal of Materials in Civil Engineering, 30(7), 04018128. https://doi.org/10.1061/(asce)mt.1943-5533.0002282

Elseifi, M. A., Al-Qadi, I. L., Flinstch, G. W., & Masson, J.-F. (2002). Viscoelastic Modeling of Straight Run and Modified Binders Using the Matching Function Approach. International Journal of Pavement Engineering, 3(1), 53–61. https://doi.org/10.1080/10298430290023476

Far, M. S. S., Underwood, B. S., Ranjithan, S. R., Kim, Y. R., & Jackson, N. (2009). Application of artificial neural networks for estimating dynamic modulus of asphalt concrete. Transportation Research Record, 2127, 173–186. https://doi.org/10.3141/2127-20

Garcia, G., & Thompson, M. (2007). Research Report FHWA-ICT-07-005: HMA Dynamic Modulus Prediction Models – A Review. Illinois Center for Transportation.

Goh, S. W., You, Z., Williams, R. C., & Li, X. (2010). Preliminary Dynamic Modulus Criteria of HMA for Field Rutting of Asphalt Pavements: Michigan's Experience. Journal of Transportation Engineering, 137(1), 37–45. https://doi.org/10.1061/(ASCE)TE.1943-5436.0000191

Huang, Y. H. (2004). Pavement Design and Analysis. United States of America: University of Kentucky.

Khattab, A. M., El-badawy, S. M., Abbas, A., Hazmi, A., & Elmwafi, M. (2014). Evaluation of Witczak E * predictive models for the implementation of AASHTOWare-Pavement ME Design in the Kingdom of Saudi Arabia. Construction and Building Materials, 64(August), 360–369.

https://doi.org/10.1016/j.conbuildmat.2014.04.066

Kim, M. (2010). Development of differential scheme micromechanics modeling framework for predictions of hot-mix asphalt (HMA) complex modulus and experimental validations. Ph.D. Dissertation, Univ. of Illinois at Urbana, Champaign, IL.

Kim, Minkyum. (2009). Development of Differential Scheme Micromechanics Modeling Framework for Predictions of Hot-Mix Asphalt (HMA) Complex Modulus and Experimental Validations. Matrix, December, 186.

Kutay, M. E., & Lanotte, M. (2020). Formulations of the Pavement Performance Prediction Models in the Mechanistic-Empirical Asphalt Pavement Analysis (MEAPA) Web Application. https://paveapps.com/meapaapp2/

Li, J., Zofka, A., & Yut, I. (2012). Evaluation of dynamic modulus of typical asphalt mixtures in Northeast US Region. Road Materials and Pavement Design, 13(2), 249–265. https://doi.org/10.1080/14680629.2012.666641

Lu, Q., Ullidtz, P., Basheer, I., Ghuzlan, K., & Signore, J. M. (2009). CalBack: Enhancing caltrans mechanistic-empirical pavement design process with new back-calculation software. Journal of Transportation Engineering, 135(7), 479–488. https://doi.org/10.1061/(ASCE)TE.1943-5436.0000010

Mateosa, A., & Soares, J. B. (2015). Validation of a dynamic modulus predictive equation on the basis of Spanish asphalt concrete mixtures. Materiales de Construccion, 65(317), e047. https://doi.org/10.3989/mc.2015.01114

MOE. (2014). Qatar Construction Specification 2014 (2nd ed.). The Ministry.

MOTC. (2015). Qatar Highway Design Manual (Issue 2). The Ministry.

Moussa, G. S., & Owais, M. (2020). Pre-trained deep learning for hot-mix asphalt dynamic modulus prediction with laboratory effort reduction. Construction and

Building Materials, 265, 120239. https://doi.org/10.1016/j.conbuildmat.2020.120239

Moussa, G. S., & Owais, M. (2021). Modeling Hot-Mix asphalt dynamic modulus using deep residual neural Networks: Parametric and sensitivity analysis study. Construction and Building Materials, 294, 123589. https://doi.org/10.1016/j.conbuildmat.2021.123589

NCHRP. (2004). Guide for Mechanistic–Empirical Design of New and Rehabilitated Pavement Structures (Final Report). Transportation Research Program, National Research Council. http://onlinelibrary.wiley.com/doi/10.1002/cbdv.200490137/abstract%5Cnhttp://scholar.google.com/scholar?hl=en&btnG=Search&q=intitle:Guide+for+Mechanistic-Empirical+Design+of+New+and+Rehabilitated+Pavement+structures#0

NCM. (n.d.). KSA Climatological Normals. Retrieved April 29, 2022, from www.ncm.gov.sa

Pellinen, Kristiina, T. (2001). Investigation of the use of dynamic modulus as an indicator of hot-mix asphalt performance. Arizona State University, Thesis (PH.

Public Work Authority. (2016). PWA Interim Advice Note No. 101 Rev 2. The Public Work Authority.

QMD. (n.d.-a). Qatar Climatological Normals. Retrieved November 14, 2021, from https://qweather.gov.qa/CAA/ClimateNormals.aspx

QMD. (n.d.-b). Qatar Climatological Normals. Retrieved November 15, 2020, from https://qweather.gov.qa/CAA/ClimateNormals.aspx

Robbins, M. M., & Timm, D. H. (2011). Evaluation of dynamic modulus predictive equations for southeastern United States asphalt mixtures. Transportation

Research Record, 2210, 122–129. https://doi.org/10.3141/2210-14

Roja, K. L., Masad, E., & Mogawer, W. (2020). Performance and blending evaluation of asphalt mixtures containing reclaimed asphalt pavement. Road Materials and Pavement Design, 0(0), 1–17. https://doi.org/10.1080/14680629.2020.1764858

Roja, L. K., Aljarrah, M. F., Sirin, O., Al-Nuaimi, N., & Masad, E. (2022). Rheological, Thermal, and Chemical Evaluation of Asphalt Binders Modified Using Crumb Rubber and Warm-Mix Additive. Journal of Materials in Civil Engineering, 34(5), 04022049.

Roja, L. K., Masad, E., & Mogawer, W. (2021). Performance and blending evaluation of asphalt mixtures containing reclaimed asphalt pavement. Road Materials and Pavement Design, 22(11), 2441–2457.

Sakhaeifar, M. S., Richard Kim, Y., & Kabir, P. (2015). New predictive models for the dynamic modulus of hot mix asphalt. Construction and Building Materials, 76, 221–231. https://doi.org/10.1016/j.conbuildmat.2014.11.011

Sebaaly, H., Riviera, P. P., Varma, S., Maina, J. W., & Santagata, E. (2020). Performance-based assessment of rutting resistance of asphalt mixes designed for hot climate regions. International Journal of Pavement Engineering, 0(0), 1–12. https://doi.org/10.1080/10298436.2020.1858484

Shen, S., Yu, H., Willoughby, K. A., Devol, J. R., & Uhlmeyer, J. S. (2013). Local practice of assessing dynamic modulus properties for Washington state mixtures. Transportation Research Record, 2373(2373), 89–99. https://doi.org/10.3141/2373-10

Shu, X., & Huang, B. (2008). Dynamic Modulus Prediction of HMA Mixtures Based on the Viscoelastic Micromechanical Model. Journal of Materials in Civil Engineering, 20(8), 530–538. https://doi.org/10.1061/(asce)0899-

1561(2008)20:8(530)

Solatifar, N. (2020). Performance Evaluation of Dynamic Modulus Predictive Models For Asphalt Mixtures. Journal of Rehabilitation in Civil Engineering, 8–3, 87–97. https://doi.org/10.22075/JRCE.2020.17391.1324

Stowe, R. L. (1969). Strength and deformation properties of granite, basalt, limestone and tuff at various loading rates. Army Engineer Waterways Experiment Station, No. AEWES-.

Yousefdoost, S., Vuong, B., Rickards, I., Armstrong, P., & Sullivan, B. (2013). Evaluation of Dynamic Modulus Predictive Models for Typical Australian Asphalt Mixes. 15th AAPA International Flexible Pavements Conference, 19, 1–18.

Zhang, B., Chen, H., Zhang, H., Kuang, D., Wu, J., & Zhang, X. (2019). A study on physical and rheological properties of rubberized bitumen modified by different methods. Materials, 12(21), 1–14. https://doi.org/10.3390/ma12213538

Zhang, C., Shen, S., & Jia, X. (2017). Modification of the Hirsch dynamic modulus prediction model for asphalt mixtures. Journal of Materials in Civil Engineering, *29*(12), 1–8. https://doi.org/10.1061/(ASCE)MT.1943-5533.0002099

Appendix A

MEAPA Output Reports

MEAPA

Mechanistic Empirical Asphalt Pavement Analysis

Detailed Analysis Report

1A - Before Calibration

User: AlTawalbeh

Report created on: 2022-03-12

Analysis run date/time: 03/12/2022 at 12:17 PM

Distress Summary

Distress	Threshold	Target Reliability	Distress @ 20.0 year(s)	Pass /Fail
IRI (in/mile)	172.0	75.0%	102.3	PASS
AC Top-Down Fatigue Cracking (ft/mile)	2000.0	75.0%	665.6	PASS
AC Bottom-up Fatigue Cracking (%)	25.0	75.0%	0.8	PASS
AC Thermal Cracking (ft/mile)	1000.0	75.0%	113.3	PASS
Total Rutting (in)	0.75	75.0%	0.2	PASS
AC Rutting (in)	0.25	75.0%	0.08	PASS
AC Reflective Cracking (%)	25.0	75.0%	0.8	PASS

Figure A1. MEAPA Distress Summary for Section 1A – Before Calibration

MEAPA

Mechanistic Empirical Asphalt Pavement Analysis

Detailed Analysis Report

1A - After Calibration

User: AlTawalbeh

Report created on: 2022-06-10

Analysis run date/time: 06/10/2022 at 02:20 PM

Distress Summary

Distress	Threshold	Target Reliability	Distress @ 20.0 year(s)	Pass /Fail
IRI (in/mile)	172.0	75.0%	103.6	PASS
AC Top-Down Fatigue Cracking (ft/mile)	2000.0	75.0%	831.6	PASS
AC Bottom-up Fatigue Cracking (%)	25.0	75.0%	0.8	PASS
AC Thermal Cracking (ft/mile)	1000.0	75.0%	113.3	PASS
Total Rutting (in)	0.75	75.0%	0.23	PASS
AC Rutting (in)	0.25	75.0%	0.11	PASS
AC Reflective Cracking (%)	25.0	75.0%	0.8	PASS

Figure A2. MEAPA Distress Summary for Section 1A – After Calibration

MEAPA

Mechanistic Empirical Asphalt Pavement Analysis

Detailed Analysis Report

1B - Before Calibration

User: AlTawalbeh

Report created on: 2022-03-12

Analysis run date/time: 03/12/2022 at 12:50 PM

Distress Summary

Distress	Threshold	Target Reliability	Distress @ 20.0 year(s)	Pass /Fail
IRI (in/mile)	172.0	75.0%	102.4	PASS
AC Top-Down Fatigue Cracking (ft/mile)	2000.0	75.0%	757.5	PASS
AC Bottom-up Fatigue Cracking (%)	25.0	75.0%	0.8	PASS
AC Thermal Cracking (ft/mile)	1000.0	75.0%	113.3	PASS
Total Rutting (in)	0.75	75.0%	0.2	PASS
AC Rutting (in)	0.25	75.0%	0.08	PASS
AC Reflective Cracking (%)	25.0	75.0%	0.8	PASS

Figure A3. MEAPA Distress Summary for Section 1B – Before Calibration

MEAPA

Mechanistic Empirical Asphalt Pavement Analysis

Detailed Analysis Report

1B - After Calibration

User: AlTawalbeh

Report created on: 2022-06-10

Analysis run date/time: 06/10/2022 at 04:32 PM

Distress Summary

Distress	Threshold	Target Reliability	Distress @ 20.0 year(s)	Pass /Fail
IRI (in/mile)	172.0	75.0%	118.6	PASS
AC Top-Down Fatigue Cracking (ft/mile)	2000.0	75.0%	1185.4	PASS
AC Bottom-up Fatigue Cracking (%)	25.0	75.0%	0.8	PASS
AC Thermal Cracking (ft/mile)	1000.0	75.0%	1878.0	FAIL
Total Rutting (in)	0.75	75.0%	0.21	PASS
AC Rutting (in)	0.25	75.0%	0.09	PASS
AC Reflective Cracking (%)	25.0	75.0%	0.8	PASS

Figure A4. MEAPA Distress Summary for Section 1B – After Calibration

MEAPA

Mechanistic Empirical Asphalt Pavement Analysis

Detailed Analysis Report

1C - Before Calibration

User: AlTawalbeh

Report created on: 2022-03-12

Analysis run date/time: 03/12/2022 at 01:25 PM

Distress Summary

Distress	Threshold	Target Reliability	Distress @ 20.0 year(s)	Pass /Fail
IRI (in/mile)	172.0	75.0%	103.3	PASS
AC Top-Down Fatigue Cracking (ft/mile)	2000.0	75.0%	994.3	PASS
AC Bottom-up Fatigue Cracking (%)	25.0	75.0%	0.8	PASS
AC Thermal Cracking (ft/mile)	1000.0	75.0%	113.3	PASS
Total Rutting (in)	0.75	75.0%	0.21	PASS
AC Rutting (in)	0.25	75.0%	0.09	PASS
AC Reflective Cracking (%)	25.0	75.0%	0.8	PASS

Figure A5. MEAPA Distress Summary for Section 1C – Before Calibration

MEAPA

Mechanistic Empirical Asphalt Pavement Analysis

Detailed Analysis Report

1C - After Calibration

User: AlTawalbeh

Report created on: 2022-06-10

Analysis run date/time: 06/10/2022 at 04:41 PM

Distress Summary

Distress	Threshold	Target Reliability	Distress @ 20.0 year(s)	Pass /Fail
IRI (in/mile)	172.0	75.0%	103.2	PASS
AC Top-Down Fatigue Cracking (ft/mile)	2000.0	75.0%	952.0	PASS
AC Bottom-up Fatigue Cracking (%)	25.0	75.0%	0.8	PASS
AC Thermal Cracking (ft/mile)	1000.0	75.0%	113.3	PASS
Total Rutting (in)	0.75	75.0%	0.21	PASS
AC Rutting (in)	0.25	75.0%	0.09	PASS
AC Reflective Cracking (%)	25.0	75.0%	0.8	PASS

Figure A6. MEAPA Distress Summary for Section 1C – After Calibration

MEAPA

Mechanistic Empirical Asphalt Pavement Analysis

Detailed Analysis Report

2A - Before Calibration

User: AlTawalbeh

Report created on: 2022-06-11

Analysis run date/time: 06/11/2022 at 12:41 PM

Distress Summary

Distress	Threshold	Target Reliability	Distress @ 20.0 year(s)	Pass /Fail
IRI (in/mile)	172.0	90.0%	121.5	PASS
AC Top-Down Fatigue Cracking (ft/mile)	2000.0	90.0%	3496.6	FAIL
AC Bottom-up Fatigue Cracking (%)	25.0	90.0%	1.5	PASS
AC Thermal Cracking (ft/mile)	1000.0	90.0%	215.3	PASS
Total Rutting (in)	0.75	90.0%	0.28	PASS
AC Rutting (in)	0.25	90.0%	0.15	PASS
AC Reflective Cracking (%)	25.0	90.0%	1.4	PASS

Figure A7. MEAPA Distress Summary for Section 2A – Before Calibration

MEAPA

Mechanistic Empirical Asphalt Pavement Analysis

Detailed Analysis Report

2A - After Calibration

User: AlTawalbeh

Report created on: 2022-06-11

Analysis run date/time: 06/11/2022 at 12:32 PM

Distress Summary

Distress	Threshold	Target Reliability	Distress @ 20.0 year(s)	Pass /Fail
IRI (in/mile)	172.0	90.0%	124.0	PASS
AC Top-Down Fatigue Cracking (ft/mile)	2000.0	90.0%	4710.8	FAIL
AC Bottom-up Fatigue Cracking (%)	25.0	90.0%	1.5	PASS
AC Thermal Cracking (ft/mile)	1000.0	90.0%	215.3	PASS
Total Rutting (in)	0.75	90.0%	0.31	PASS
AC Rutting (in)	0.25	90.0%	0.19	PASS
AC Reflective Cracking (%)	25.0	90.0%	1.4	PASS

Figure A8. MEAPA Distress Summary for Section 2A – After Calibration

MEAPA

Mechanistic Empirical Asphalt Pavement Analysis

Detailed Analysis Report

2B - Before Calibration

User: AlTawalbeh

Report created on: 2022-06-09

Analysis run date/time: 06/09/2022 at 02:14 PM

Distress Summary

Distress	Threshold	Target Reliability	Distress @ 20.0 year(s)	Pass /Fail
IRI (in/mile)	172.0	90.0%	122.6	PASS
AC Top-Down Fatigue Cracking (ft/mile)	2000.0	90.0%	4595.7	FAIL
AC Bottom-up Fatigue Cracking (%)	25.0	90.0%	1.5	PASS
AC Thermal Cracking (ft/mile)	1000.0	90.0%	215.3	PASS
Total Rutting (in)	0.75	90.0%	0.28	PASS
AC Rutting (in)	0.25	90.0%	0.16	PASS
AC Reflective Cracking (%)	25.0	90.0%	1.4	PASS

Figure A9. MEAPA Distress Summary for Section 2B – Before Calibration

MEAPA

Mechanistic Empirical Asphalt Pavement Analysis

Detailed Analysis Report

2B - After Calibration

User: AlTawalbeh

Report created on: 2022-06-10

Analysis run date/time: 06/10/2022 at 05:12 PM

Distress Summary

Distress	Threshold	Target Reliability	Distress @ 20.0 year(s)	Pass /Fail
IRI (in/mile)	172.0	90.0%	121.2	PASS
AC Top-Down Fatigue Cracking (ft/mile)	2000.0	90.0%	3941.2	FAIL
AC Bottom-up Fatigue Cracking (%)	25.0	90.0%	1.4	PASS
AC Thermal Cracking (ft/mile)	1000.0	90.0%	215.3	PASS
Total Rutting (in)	0.75	90.0%	0.26	PASS
AC Rutting (in)	0.25	90.0%	0.13	PASS
AC Reflective Cracking (%)	25.0	90.0%	1.4	PASS

Figure A10. MEAPA Distress Summary for Section 2B – After Calibration

MEAPA

Mechanistic Empirical Asphalt Pavement Analysis

Detailed Analysis Report

1C - Before Calibration

User: AlTawalbeh

Report created on: 2022-03-12

Analysis run date/time: 03/12/2022 at 01:25 PM

Distress Summary

Distress	Threshold	Target Reliability	Distress @ 20.0 year(s)	Pass /Fail
IRI (in/mile)	172.0	75.0%	103.3	PASS
AC Top-Down Fatigue Cracking (ft/mile)	2000.0	75.0%	994.3	PASS
AC Bottom-up Fatigue Cracking (%)	25.0	75.0%	0.8	PASS
AC Thermal Cracking (ft/mile)	1000.0	75.0%	113.3	PASS
Total Rutting (in)	0.75	75.0%	0.21	PASS
AC Rutting (in)	0.25	75.0%	0.09	PASS
AC Reflective Cracking (%)	25.0	75.0%	0.8	PASS

Figure A11. MEAPA Distress Summary for Section 1C – Before Calibration

MEAPA

Mechanistic Empirical Asphalt Pavement Analysis

Detailed Analysis Report

1C - After Calibration

User: AlTawalbeh

Report created on: 2022-06-10

Analysis run date/time: 06/10/2022 at 04:41 PM

Distress Summary

Distress	Threshold	Target Reliability	Distress @ 20.0 year(s)	Pass /Fail
IRI (in/mile)	172.0	75.0%	103.2	PASS
AC Top-Down Fatigue Cracking (ft/mile)	2000.0	75.0%	952.0	PASS
AC Bottom-up Fatigue Cracking (%)	25.0	75.0%	0.8	PASS
AC Thermal Cracking (ft/mile)	1000.0	75.0%	113.3	PASS
Total Rutting (in)	0.75	75.0%	0.21	PASS
AC Rutting (in)	0.25	75.0%	0.09	PASS
AC Reflective Cracking (%)	25.0	75.0%	0.8	PASS

Figure A12. MEAPA Distress Summary for Section 1C – After Calibration

Appendix B

Job Mix Formula Sample Report

Fugro Peninsular
Pavement Services Division
Volumetric Mix Design Services

Volumetric Mix Design Process Diagram

Overseeing Engineer: Zahi Chamoun

	Laboratory Volumetric Mix Design Stages
T0: Preliminaries	• Review of Applicable Specification • Project Requirements (traffic type / surface texture) • Production considerations (available materials / screens) • Binder content restrictions • Objective of the mix design • Material sampling
T1: Material Verification	• Aggregate compliance testing (stock-piles / hot-bins) • Binder testing (PEN / PMB) • Binder Mixing & Compaction temperature • Aggregate sieve analysis / specific gravities / unit weights
T2: Selection of Gradation	• Contractor preference from past experiences • Bailey Aggregate Packing Method employed • Initial trials for volumetric feasibility / binder content indication • Gradation review by the Contractor
T3: Selection of Binder Content	• Volumetric curves at 4 – 6 binder contents • Verification of design binder content • Including expected volumetric property ranges given specification production tolerances
T4: Moisture Susceptibility	• Tensile Strength Ratio (TSR) for Superpave • Retained Stability for Marshall
	Supplemental Plant Verification Stages
T5: Plant Verification	• Can the designed aggregate structure be achieved in the plant? • Does the binder content require adjustment for production?
T6: Performance	• Mechanistic Performance testing – Dynamic Modulus |E*| • Rutting Indicators – Flow Number (repeated load triaxle testing) • Rutting Indicators – Hamburg Wheel Track Testing (HWTT) at local climatic conditions (76degC)
Notes:	• Mix design process is the same for Marshall or Superpave Volumetric Mix Designs • It is recommended to carry out performance testing on plant produced material when using PMB asphalt binders • T5 and T6 are not required for a Volumetric Mix Design, but provide supplemental information beneficial to projects, especially projects with high traffic loads where mixture performance is more critical

Page 1

Figure B1. JMF Testing Plan

FUGRO PENINSULAR
Geotechnical, Material Testing, Engineers,
Foundation Testing, Pavement Services

Pavements Services Division
Asphalt Mix Design Services

FUGRO

SUPERPAVE MIX DESIGN REPORT

JMF No.: QTR/119
Report No.: 00038

Plant:	MIDMAC COLAS	**Design ESAL:**	Not Applicable (N/A)
Designer:	Zahi Chamoun	**Asphalt Grade:**	PG 76E-10
Date:	07-Jan-19	**Aggregate Source:**	Village Trading Group
NMAS:	25.0 mm	**Asphalt Source:**	MEMBCO
Material Type:	Not Applicable (N/A)	**Binder Content:**	4.1%

Technical References and Applicable Standards

AASHTO PP60	Standard Practice for Preparation of Cylindrical Performance Test Specimens Using the Superpave Gyratory Compactor (SGC)
AASHTO PP61	Standard Practice for Developing Dynamic Modulus Master Curves for Asphalt Mixtures Using the Asphalt Mixture Performance Tester (AMPT)
AASHTO R28	Standard Practice for Accelerated Aging of Asphalt Binder Using a Pressurized Aging Vessel (PAV)
AASHTO T19	Standard Method of Test for Bulk Density ("Unit Weight") and Voids in Aggregate
AASHTO T44	Standard Method of Test for Solubility of Bituminous Materials
AASHTO T48	Standard Method of Test for Flash and Fire Points by Cleveland Open Cup
AASHTO T55	Standard Method of Test for Water in Petroleum Products and Bituminous Materials by Distillation
AASHTO T228	Standard Method of Test for Specific Gravity of Semi-Solid Asphalt Materials
AASHTO T240	Standard Method of Test for Effect of Heat and Air on a Moving Film of Asphalt Binder (Rolling Thin-Film Oven Test)
AASHTO T283	Resistance of Compacted Hot-Mix Asphalt (HMA) to Moisture-Induced Damage
AASHTO T313	Standard Method of Test for Determining the Flexural Creep Stiffness of Asphalt Binder Using the Bending Beam Rheometer (BBR)
AASHTO T315	Standard Method of Test for Determining the Rheological Properties of Asphalt Binder Using a Dynamic Shear Rheometer (DSR)
AASHTO T316	Standard Method of Test for Viscosity Determination of Asphalt Binder Using Rotational Viscometer
AASHTO T350	Standard Method of Test for Multiple Stress Creep Recovery (MSCR) Test of Asphalt Binder Using a Dynamic Shear Rheometer (DSR)
AASHTO TP79	Standard Method of Test for Determining the Dynamic Modulus and Flow Number for Asphalt Mixtures Using the Asphalt Mixture Performance Tester (AMPT)
ASTM D75	Standard Practice for Sampling Aggregates
ASTM C88	Standard Test Method for Soundness of Aggregates by Use of Sodium Sulfate or Magnesium Sulfate
ASTM C117	Standard Test Method for Materials Finer than 75-μm (No. 200) Sieve in Mineral Aggregates by Washing
ASTM C127	Standard Test Method for Density, Relative Density (Specific Gravity) and Absorption of Coarse Aggregate
ASTM C128	Standard Test Method for Density, Relative Density (Specific Gravity), and Absorption of Fine Aggregate
ASTM C131	Standard Test Method for Resistance to Degradation of Small-Size Coarse Aggregate by Abrasion and Impact in the Los Angeles Machine
ASTM C136	Standard Test Method for Sieve or Screen Analysis of Fine and Coarse Aggregates
ASTM C142	Standard Test Method for Clay Lumps and Friable Particles in Aggregates
ASTM C183	Standard Practice for Sampling and the Amount of Testing of Hydraulic Cement
ASTM D546	Standard Test Method for Sieve Analysis of Mineral Filler for Bituminous Paving Mixtures
ASTM C566	Standard Test Method for Total Evaporable Moisture Content of Aggregate by Drying
ASTM D854	Standard Test Methods for Specific Gravity of Soil Solids by Water Pycnometer
ASTM D979	Standard Practice for Sampling Bituminous Paving Mixtures
ASTM D1073	Standard Specification for Fine Aggregate for Bituminous Paving Mixtures
ASTM D2172	Standard Test Method for Quantitative Extraction of Bitumen from Bituminous Paving Mixtures
ASTM D2419	Standard Test Method for Sand Equivalent Value of Soils and Fine Aggregate
ASTM D2726	Standard Test Method for Bulk Specific Gravity and Density of Non-Absorptive Compacted Bituminous Mixtures
ASTM D3203	Standard Test Method for Percent Air Voids in Compacted Dense and Open Bituminous Paving Mixtures
ASTM D4318	Standard Test Methods for Liquid Limit, Plastic Limit, and Plasticity Index of Soils
ASTM D4791	Standard Test Method for Flat Particles, Elongated Particles, or Flat and Elongated Particles in Coarse Aggregate
ASTM D5821	Standard Test Method for Determining the Percentage of Fractured Particles in Coarse Aggregate
ASTM D6925	Standard Test Method for Preparation and Determination of the Relative Density of Hot Mix Asphalt (HMA) Specimens by Means of the Superpave Gyratory Compactor
ASTM D6857	Standard Test Method for Maximum Specific Gravity and Density of Bituminous Paving Mixtures Using Automatic Vacuum Sealing Method
ASTM E11	Standard Specification for Woven Wire Test Sieve Cloth and Test Sieves
A.I. SP-2	Superpave Mix Design Manual
NCHRP 648	Mixing and Compaction Temperatures of Asphalt Binders in Hot-Mix Asphalt
ASTM D242	Standard Specification for Mineral Filler for Bituminous Paving Mixtures
AASHTO M323	Standard Specification for Superpave Volumetric Mix Design
AASHTO M332	Standard Specification for Performance-Graded Asphalt Binder Using Multiple Stress Creep Recovery (MSCR) Test
AASHTO R29	Standard Practice for Grading or Verifying the Performance Grade (PG) of an Asphalt Binder
Specification	PROJECT SPECIFICATION; SECTION 02401; PLANT MIX BITUMINOUS PAVEMENT (AIRFIELD); NEW DOHA INTERNATIONAL AIRPORT; Doc. No. 25045-27-3PS-02401; Rev. 08 Dated 22-Mar-2015

Prepared By: Zahi Chamoun, Project Engineer

Reviewed By: Quality Assurance / Quality Control Dept.

C.R.: 16522 Doha-Qatar

C.R. No.: 16522, P.O. Box 47 167, Doha, Qatar, pavements.fme@fugro.com
Reproduction of this report must be in full, prior written approval from Fugro Peninsular is to be obtained.

V1R2 150405
1 of 18

Page 2

Figure B2. Technical References and Applicable Standards

FUGRO PENINSULAR
Geotechnical, Material Testing, Engineers,
Foundation Testing, Pavement Services

Pavements Services Division
Asphalt Mix Design Services

SUPERPAVE JOB MIX FORMULA REPORT

JMF No.: QTR/119
Report No.: 00038

Plant:	MIDMAC COLAS	**Design ESAL:**	Not Applicable (N/A)
Designer:	Zahi Chamoun	**Asphalt Grade:**	PG 76E-10
Date:	07-Jan-19	**Aggregate Source:**	Village Trading Group
NMAS:	25.0 mm	**Asphalt Source:**	MEMBCO
Material Type:	Not Applicable (N/A)	**Binder Content:**	4.1%

CONSTITUENT MATERIAL SOURCE PROPERTIES

Sample ID	Supplier	Material (mm)	JMF, %	G_{sb}	G_{sa}	Absorption	Fracture Faces	Flat & Elongate
18-11603	Village Trading Group	22-37.5	20.6	2.888	2.928	0.5	100	1
18-11604	Village Trading Group	12-22	24.6	2.919	2.980	0.7	100	1
18-11605	Village Trading Group	7-12	19.4	2.902	2.974	0.8	100	NIL
18-11606	Village Trading Group	4.5-7	5.4	2.883	2.963	0.9	-	-
18-11602	Village Trading Group	0-4.5	28.3	-	2.953	-	-	-
				-		-	-	-
							(min 100)	*(max 8)*

(SPECIFICATION LIMIT)

Sample ID	Supplier	Material (Grade)	Lab Temp, °C Mixing	Lab Temp, °C Comp.	JMF, %	G_b	Modifier Type
18-11587	MEMBCO	PG 76 - 10 "E"	175	162	4.1	1.03	PMB
					(4.0 - 5.5)		

(SPECIFICATION LIMIT)

DESIGN AGGREGATE STRUCTURE

37.5 mm	25.0 mm	19.0 mm	12.5 mm	9.5 mm	4.75 mm	2.36 mm	1.18 mm	0.600 mm	0.300 mm	0.150 mm	0.075 mm
100.0	95.0	82.0	65.0	52.0	34.0	21.0	13.0	10.0	7.0	6.0	4.4
	(100)	*(90-100)*	*(<90)*			*(23-49)*					*(2-8)*

(SPECIFICATION LIMIT)

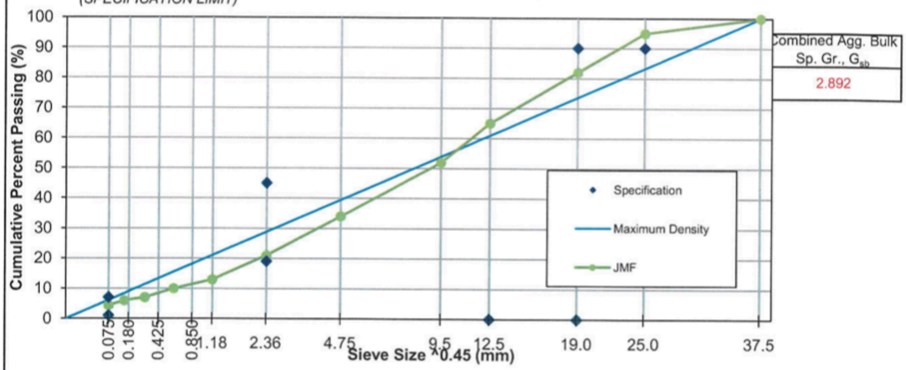

DESIGN MIXTURE LABORATORY CHARACTERISTICS (GYRATORY)

Design ESALs	Gyrations @ N_{ini}	Gyrations @ N_{des}	Gyrations @ N_{max}	Max Density, G_{mm}	Density @ N_{des}
N/A	8	100	160	2.721	2.611
TSR	**% VIM @ Nini**	**% VIM @ Ndes**	**% VIM @ Nmax**	**% VMA @ Ndes**	**% VFA @ Ndes**
97.0	13.5	4.0	2.9	13.4	70
(80%)	*(min 12)*	*(4.0)*	*(min 2)*	*(min 13)*	*(65 - 75)*

(SPECIFICATION LIMIT)

Prepared By: Zahi Chamoun
Project Engineer

Reviewed By: Quality Assurance / Quality Control Dept.

C.R. No.: 16522, P.O. Box 47 167, Doha, Qatar, pavements.fme@fugro.com

V1R2 150405
3 of 18

Page 3

Figure B3. Material Source Properties

FUGRO PENINSULAR
Geotechnical, Material Testing, Engineers,
Foundation Testing, Pavement Services

Pavements Services Division
Asphalt Mix Design Services

FUGRO

AGGREGATE GRADATION .45 POWER PLOTS		JMF No.:	QTR/119
		Report No.:	00038
Plant:	MIDMAC COLAS	Design ESAL:	Not Applicable (N/A)
Designer:	Zahi Chamoun	Asphalt Grade:	PG 76E-10
Date:	07-Jan-19	Aggregate Source:	Village Trading Group
NMAS:	25.0 mm	Asphalt Source:	MEMBCO
Material Type:	Not Applicable (N/A)	Binder Content:	4.1%

AGGREGATE JOB MIX FORMULA GRADATION WITH CONSTRUCTION TOLERANCES

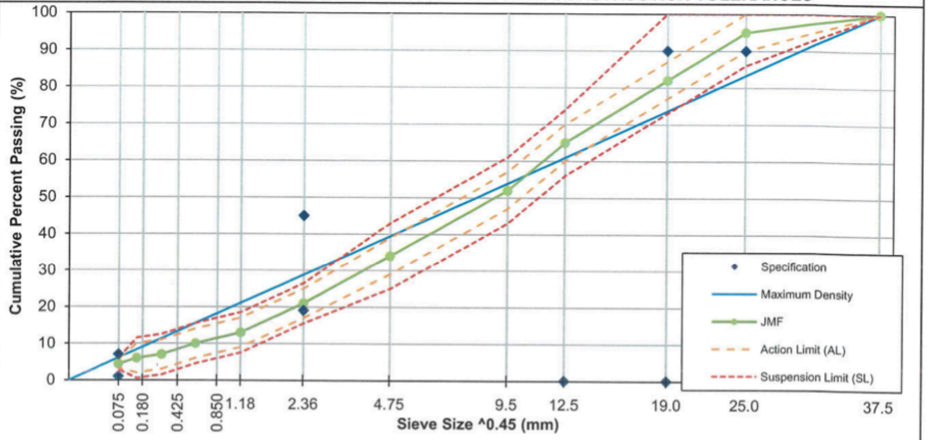

Prepared By:	Zahi Chamoun Project Engineer	Reviewed By:	Quality Assurance / Quality Control Dept.

C.R.: 16522
Doha-Qatar
Fugro Peninsular

Figure B4. JMF Gradation Chart

FUGRO PENINSULAR
Geotechnical, Material Testing, Engineers,
Foundation Testing, Pavement Services

Pavements Services Division
Asphalt Mix Design Services

FUGRO

STOCK-PILE AGGREGATE PHYSICAL PROPERTIES

JMF No.: QTR/119
Report No.: 00038

Plant:	MIDMAC COLAS	**Design ESAL:**	Not Applicable (N/A)
Designer:	Zahi Chamoun	**Asphalt Grade:**	PG 76E-10
Specification:	07-Jan-19	**Aggregate Source:**	Village Trading Group
NMAS:	25.0 mm	**Asphalt Source:**	MEMBCO
Material Type:	Not Applicable (N/A)	**Design Binder Content:**	4.1%

Sample ID	Material (mm)	Stock-pile Source	Sampling Date	Producer Logo
18-11593	32mm	Village Trading Group	01-Dec-18	midmac مدماك COLAS
18-11594	20mm	Village Trading Group	01-Dec-18	
18-11595	10mm	Village Trading Group	01-Dec-18	
18-11596	0-5mm	Village Trading Group	01-Dec-18	

Aggregate Stock-pile Grading (ASTM C117 / ASTM C136)

Metric Sieve Size (mm)	32mm	20mm	10mm	0-5mm	Specs Min	Specs Max
37.5	100	100	100	100		
25.0	74	100	100	100		
19.0	20	95	100	100		
12.5	5	43	100	100		
9.5	4	8	97	100		
4.75	3	2	44	99		
2.36	3	2	12	72		
0.600	3	2	6	37		
0.300	2	2	5	28		
0.150	2	2	4	21		
0.075	1.9	1.4	3.9	16.3		

AGGREGATE PHYSICAL PROPERTIES

Parameter (Standard of Test)	32mm	20mm	10mm	0-5mm	Specification Min	Specification Max
G_{sb} (C127/C128)	2.897	2.930	2.882	2.854		
G_{sa} (C127/C128/D854)	2.932	2.974	2.942	2.943		
Absorption (C127/C128)	0.4	0.5	0.7	1.1		
Rodded Unit Wt (T19)	1,720	1,710	1,630	1,510		
Shovel Unit Wt (T19)	1,640	1,650	1,610	1,320		
Plastic Limit (D4318)				NP		
Liquid Limit (D4318)				ND		25
Plasticity Index (D4318)				ND		6
Percent Wear (C131)	8	12	17			40
Soundness (C88)	0	1	1	2		12 / 18
Clay & Friable (C142)				None		1
Sand Equiv. (D2419)				56	50	
Organic Impurities (C40)						None
Acid soluble Cl- content (BS 1377 Part 3)				0.04		0.1%
Acid soluble SO3- content (BS 1377 Part 3)				0.13		0.5%
Flat & Elongated (D4791)	NIL	NIL	1			8 (5:1)
Fractured Faces (D5821)	100	100	100		75	

Prepared By:	Zahi Chamoun Project Engineer	Reviewed By:	Quality Assurance / Quality Control Dept.

C.R. No.: 16522, P.O. Box 47 167, Doha, Qatar, pavements.fme@fugro.com

V1R2 150405
6 of 18

Page 5

Figure B5. Stockpile Aggregate Phyiscal Propoerites

FUGRO PENINSULAR

Geotechnical, Material Testing, Engineers, Foundation Testing, Pavement Services

Pavements Services Division
Asphalt Mix Design Services

HOT-BIN AGGREGATE AND JMF TRIAL GRADATIONS

JMF No.: QTR/119
Report No.: 00038

Plant:	MIDMAC COLAS	**Design ESAL:**	Not Applicable (N/A)
Designer:	Zahi Chamoun	**Asphalt Grade:**	PG 76E-10
Date	07-Jan-19	**Aggregate Source:**	Village Trading Group
NMAS:	25.0 mm	**Asphalt Source:**	MEMBCO
Material Type:	Not Applicable (N/A)	**Design Binder Content:**	4.1%

Sample ID	Material	JMF Trial 1	JMF Trial 2	JMF Trial 3	Sampling Date	Producer Logo
18-11603	22-37.5mm	18.3	30.0	20.6	01-Dec-18	
18-11604	12-22mm	20.0	25.0	24.6	01-Dec-18	
18-11605	7-12mm	15.0	7.0	19.4	01-Dec-18	
18-11606	4.5-7mm	5.0	6.0	5.4	01-Dec-18	
18-11602	0-4.5mm	40.0	30.0	28.3	01-Dec-18	
18-11607	Filler	1.7	2.0	1.7	01-Dec-18	

Aggregate Hot-bin Grading (C117 / C136 / D546) and Combinded Grading

Sieve	Hot-bin Gradations						JMF	JMF	JMF	Superpave (25mm NMAS)	
Metric	22-37.5mm	12-22mm	7-12mm	4.5-7mm	0-4.5mm	Filler	Trial 1	Trial 2	Trial 3	Min	Max
37.5	100	100	100	100	100	100	100	100	100	100	
25.0	75	100	100	100	100	100	95	93	95	90	100
19.0	17	94	100	100	100	100	84	74	82		90
12.5	3	39	100	100	100	100	70	56	65		
9.5	1	3	82	100	100	100	60	45	52		
4.75	1	1	2	51	100	100	45	36	34		
2.36	1	1	2	2	65	100	28	22	21	19	45
1.18	1	1	1	1	38	100	18	14	13		
0.850	1	1	1	1	31	100	15	12	11		
0.600	1	1	1	1	25	100	12	10	10		
0.425	1	1	1	1	21	100	11	9	8		
0.300	1	1	1	1	18	100	9	8	7		
0.180	1	1	1	1	14	100	8	7	6		
0.150	1	1	1	1	12	99	7	6	6		
0.075	0.4	0.9	1.2	1.1	7.8	91.0	5.2	4.7	4.4	1	7

0.45 Power Plot of Job-Mix Formula

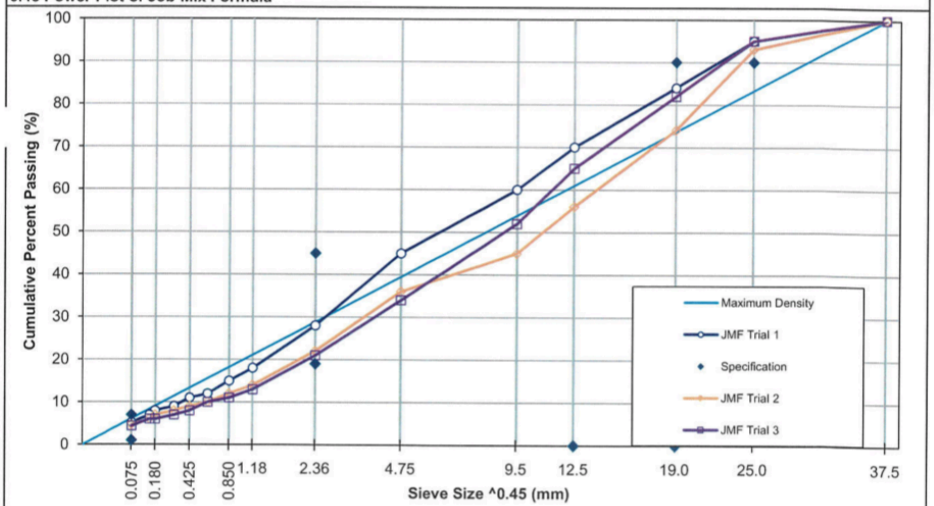

Prepared By: Zahi Chamoun, Project Engineer

Reviewed By: Quality Assurance / Quality Control Dept.

C.R. No.: 16522, P.O. Box 47 167, Doha, Qatar, pavements.fme@fugro.com

Ver 01 Rev 00
7 of 18

Page 6

Figure B6. Hot-Bin Aggregate and Trial Gradations

FUGRO PENINSULAR
Geotechnical, Material Testing, Engineers,
Foundation Testing, Pavement Services

Pavements Services Division
Asphalt Mix Design Services

SUPERPAVE DESIGN BINDER CONTENT VERIFICATION

JMF No.: QTR/119
Report No.: 00038

Plant:	MIDMAC COLAS	**Design ESAL:**	Not Applicable (N/A)
Designer:	Zahi Chamoun	**Asphalt Grade:**	PG 76E-10
Date:	07-Jan-19	**Aggregate Source:**	Village Trading Group
NMAS:	25.0 mm	**Asphalt Source:**	MEMBCO
Material Type:	Not Applicable (N/A)	**Design Binder Content:**	4.1%

Volumetric Mix Design Inputs

Parameter / Standard of Test		2-37.5mr	12-22mm	7-12mm	4.5-7mm	0-4.5mm	Filler		QCS 2014 Min	QCS 2014 Max
Agg Bulk SG (G_{sb})	C127 / C128	2.888	2.919	2.902	2.888	2.868				
Agg Apparent SG (G_{sa})	C127/C128/D854	2.928	2.980	2.974	2.966	2.954	2.892			
Superpave Combined Agg Bulk SG (G_{sb})		2.888								
Superpave Combined Agg App SG (G_{sa})		2.957								

Volumetric Mix Design Inputs - 18-12213

Sample ID: 18-12213 | Binder Content: 4.3 | Gmm: 2.713

	Dry Weight	Weight in H_2O	SSD Weight	G_{mb} @ $N_{compact}$	Height @ N_9	Height @ N_{100}	Height @ N_{160}	%G_{mm} @ N_9	%G_{mm} @ N_{100}	%G_{mm} @ N_{160}	VIM @ $N_{compact}$	VMA @ N_{100}	VFA @ N_{100}
/1 N_{des}	5090.1	3163.2	5099.2	2.629	124.2	112.6		87.9	96.9	-	3.1	12.9	76.0
/2 N_{des}	5096.2	3161.3	5104.4	2.623	125.3	113.7		87.7	96.7	-	3.3	13.1	74.8
/3 N_{des}	5109.8	3172.9	5117.4	2.628	124.2	112.6		87.8	96.9	-	3.1	12.9	76.0
	Dry Weight	Weight in H_2O	SSD Weight	G_{mb} @ $N_{compact}$	Height @ N_9	Height @ N_{100}	Height @ N_{160}	%G_{mm} @ N_9	%G_{mm} @ N_{100}	%G_{mm} @ N_{160}	VIM @ $N_{compact}$	VMA @ N_{100}	VFA @ N_{100}
/4 Nmax	5103.4	3193.6	5106.1	2.668	124.1	112.3	110.8	87.8	97.0	98.3	3.0	-	-
/5 Nmax	5088.5	3182.4	5092.7	2.664	123.4	112.7	111.3	88.6	97.0	98.2	3.0	-	-
Average Volumetric Properties @ Ndes								87.8	96.8	-	3.2	-	-
Average Volumetric Properties @ Nmax								88.2	97.0	98.3	3.0	-	-

Volumetric Mix Design Inputs

Parameter / Standard of Test		2-37.5mr	12-22mm	7-12mm	4.5-7mm	0-4.5mm	Filler		QCS 2014 Min	QCS 2014 Max
Agg Bulk SG (G_{sb})	C127 / C128	2.888	2.919	2.902	2.888	2.868				
Agg Apparent SG (G_{sa})	C127/C128/D854	2.928	2.980	2.974	2.966	2.954	2.892			
Superpave Combined Agg Bulk SG (G_{sb})		2.891								
Superpave Combined Agg App SG (G_{sa})		2.953								

Volumetric Mix Design Inputs - 18-12212

Sample ID: 18-12212 | Binder Content: 4.3 | Gmm: 2.715

	Dry Weight	Weight in H_2O	SSD Weight	G_{mb} @ $N_{compact}$	Height @ N_9	Height @ N_{100}	Height @ N_{160}	%G_{mm} @ N_9	%G_{mm} @ N_{100}	%G_{mm} @ N_{160}	VIM @ $N_{compact}$	VMA @ N_{100}	VFA @ N_{100}
/1 N_{des}	5071.0	3177.3	5078.5	2.667	125.3	113.6		89.1	98.2	-	1.8	11.7	84.6
/2 N_{des}	5085.9	3189.5	5095.5	2.668	125.4	113.0		88.6	98.3	-	1.7	11.7	85.5
/3 N_{des}	5090.9	3191.9	5098.3	2.670	126.4	113.3		88.2	98.3	-	1.7	11.6	85.3
	Dry Weight	Weight in H_2O	SSD Weight	G_{mb} @ $N_{compact}$	Height @ N_9	Height @ N_{100}	Height @ N_{160}	%G_{mm} @ N_9	%G_{mm} @ N_{100}	%G_{mm} @ N_{160}	VIM @ $N_{compact}$	VMA @ N_{100}	VFA @ N_{100}
/4 Nmax	5090.9	3204.6	5098.9	2.687	126.7	114.3	112.7	88.0	97.6	99.0	2.4	-	-
/5 Nmax	5105.6	3216.6	5112.1	2.694	125.2	112.6	111.2	88.1	98.0	99.3	2.0	-	-
Average Volumetric Properties @ Ndes								88.6	98.3	-	1.7	-	-
Average Volumetric Properties @ Nmax								88.1	97.8	99.2	2.2	-	-

Prepared By: Zahi Chamoun
Project Engineer

Reviewed By: Quality Assurance /
Quality Control Dept.

C.R. : 16522
Doha-Qatar

C.R. No.: 16522, P.O. Box 47 167, Doha, Qatar, pavements.fme@fugro.com

Ver 01 Rev 00
8 of 18

Page 7

Figure B7. Superpave Design Binder Content Verfication

FUGRO PENINSULAR
Geotechnical, Material Testing, Engineers, Foundation Testing, Pavement Services

Pavements Services Division
Asphalt Mix Design Services

FUGRO

ASPHALT BINDER PROPERTIES

JMF No.: QTR/119
Report No.: 00038

Plant:	MIDMAC COLAS	**Design ESAL:**	Not Applicable (N/A)
Designer:	Zahi Chamoun	**Asphalt Grade:**	PG 76E-10
Date:	07-Jan-19	**Aggregate Source:**	Village Trading Group
NMAS:	25.0 mm	**Asphalt Source:**	MEMBCO
Material Type:	Asphalt Binder	**Binder Content:**	4.1%
Sample ID:	18-11587		

AASHTO M332 SCREENING TEST RESULTS

Test Method	Parameter	Test Temperature		Test Result		Specification		
AASHTO T44	Solubility	-	°C	100	%	99.0	%	min
AASHTO T55	Water Content	-	°C		%	0.0	%	max
250 μm Sieve Test	Particles	160	°C	0.80	No.	0.0	No	max

PG VERIFICATION - AASHTO M332 (TABLE 1) TEST RESULTS

Test Method	Parameter	Test Temperature		Test Result		Specification		
AASHTO T48	Temp	-	°C	318	°C	230	°C	min
AASHTO T316	Viocosity	135	°C	2.2	Pa·s	3	Pa·s	max
AASHTO T315	$G^*/\sin\delta$	76	°C	1.90	kPa	1.00	kPa	min
AASHTO T240	Mass Δ	163	°C	-0.08	%	1.00	%	max
AASHTO T350	$J_{nr3.2}$	76	°C	0.261	kPa-1	1.0	kPa^{-1}	max
	J_{nrdiff}			176.0	%	75	%	max
AASHTO R28	Temp	110	°C	110	-	110	°C	-
AASHTO T315	$G^*\sin\delta$	37	°C	998	kPa	6,000	kPa	max
AASHTO T313	S	0	°C	37.0	MPa	300	MPa	max
	m-value		°C	0.391	-	0.300	-	min
AASHTO T314	Fail ε	Not Required, footnote h				1	%	min

Note: As per speciifcation if Jnr3.2 < 0.5 then Jnrdiff requirement is waived

STORAGE STABILITY - ASTM D 7173 AND AASHTO T53 TEST RESULTS

Top Residue	DSR Test (G* value)	1.6
Bottom Residue		1.5
Difference		4.7%

SPECIFIC GRAVITY - AASHTO T228 TEST RESULT

1.030

LABORATORY MIXING AND COMPACTION TEMPERATURE - NCHRP 648 PHASE ANGLE METHOD RESULT

Mixing Temperature (ºC)	175
Compaction Temperature (ºC)	162

Prepared By: Zahi Chamoun, Project Engineer

Reviewed By: Quality Assurance / Quality Control Dept.

C.R. No.: 16522, P.O. Box 47 167, Doha, Qatar, pavements.fme@fugro.com

V1R2 150405
9 of 18

Page 8

Figure B8. Asphalt Binder Properties - 1

FUGRO PENINSULAR
Geotechnical, Material Testing, Engineers,
Foundation Testing, Pavement Services

Pavements Services Division
Asphalt Mix Design Services

FUGRO

ASPHALT BINDER PROPERTIES

JMF No.: QTR/119
Report No.: 00038

Plant:	MIDMAC COLAS	**Design ESAL:**	Not Applicable (N/A)
Designer:	Zahi Chamoun	**Asphalt Grade:**	PG 76E-10
Date:	07-Jan-19	**Aggregate Source:**	Village Trading Group
NMAS:	25.0 mm	**Asphalt Source:**	MEMBCO
Material Type:	Asphalt Binder	**Binder Content:**	4.1%
Sample ID:	18-08088 (PG64S-22)		

AASHTO M332 SCREENING TEST RESULTS

Test Method	Parameter	Test Temperature		Test Result		Specification		
AASHTO T44	Solubility	-	°C	100	%	99.0	%	min
AASHTO T55	Water Content	-	°C		%	0.0	%	max
250 µm Sieve Test	Particles	160	°C	0.20	No.	0.0	No	max

PG VERIFICATION - AASHTO M332 (TABLE 1) TEST RESULTS

Test Method	Parameter	Test Temperature		Test Result		Specification		
AASHTO T48	Temp	-	°C	334	°C	230	°C	min
AASHTO T316	Viscosity	135	°C	0.4	Pa·s	3.00	Pa·s	max
AASHTO T315	$G^*/sin\delta$	64	°C	-	kPa	1.00	kPa	min
AASHTO T240	Mass Δ	163	°C	0.03	%	1.00	%	max
AASHTO T350	$J_{nr3.2}$	64	°C	3.366	kPa-1	Report only		
	J_{nrdiff}			15.0	%	Report only		
AASHTO R28	Temp	100	°C	100	-	100	°C	-
AASHTO T315	$G^*sin\delta$	25	°C	4,597	kPa	6,000	kPa	max
AASHTO T313	S	-12	°C	176	MPa	300	MPa	max
	m-value		°C	0.315	-	0.300	-	min
AASHTO T314	Fail ε	Not Required, footnote h				1	%	min

Note: As per speciifcation if Jnr3.2 < 0.5 then Jnrdiff requirement is waived

STORAGE STABILITY - ASTM D 7173 AND AASHTO T53 TEST RESULTS

Top Residue	DSR Test (G* value)	1.38
Bottom Residue		1.35
Difference		2.2%

SPECIFIC GRAVITY - AASHTO T228 TEST RESULT

1.030

LABORATORY MIXING AND COMPACTION TEMPERATURE - NCHRP 648 PHASE ANGLE METHOD RESULT

Mixing Temperature (ºC)	175
Compaction Temperature (ºC)	162

Prepared By: Zahi Chamoun
Engineer IV

س.ت : ١٦٥٢٢
الدوحة - قطر
C.R. : 16522
Doha-Qatar

Reviewed By: Quality Assurance /
Quality Control Dept.

C.R. No.: 16522, P.O. Box 47 167, Doha, Qatar, pavements.fme@fugro.com

V1R2 150405
10 of 18

Page 9

Figure B9. Asphalt Binder Properties - 2

FUGRO PENINSULAR

Geotechnical, Material Testing, Engineers,
Foundation Testing, Pavement Services

Pavements Services Division
Asphalt Mix Design Services

FUGRO

MIX DESIGN VOLUMETRIC DATA

JMF No.: QTR/119
Report No.: 00038

Plant:	MIDMAC COLAS	**Design ESAL:**	Not Applicable (N/A)
Designer:	Zahi Chamoun	**Asphalt Grade:**	PG 76E-10
Date:	07-Jan-19	**Aggregate Source:**	Village Trading Group
NMAS:	25.0 mm	**Asphalt Source:**	MEMBCO
Material Type:	Not Applicable (N/A)	**Binder Content:**	4.1%

Blend	Sample ID		18-11828		P_b, %	3.0	G_{mm}	/1	2.775	/2	2.774	Avg	2.775
JMF	Dry Weight	Weight in H_2O	SSD Weight	G_{mb} @ $N_{compact}$	Height @ N_{ini}	Height @ N_{des}	Height @ N_{max}	$\%G_{mm}$ @ N_{ini}	$\%G_{mm}$ @ N_{des}	$\%G_{mm}$ @ N_{max}	VIM @ $N_{compact}$	VMA @ N_{des}	VFA @ N_{des}
Spec 1	5092.1	3153.3	5140.7	2.562	129.5	117.5	-	83.8	92.3	-	7.7	14.1	45.4
Spec 2	5090.6	3153.6	5134.2	2.570	129.2	117.2	-	84.0	92.6	-	7.4	13.8	46.4
Spec 3	5097.2	3160.6	5138.2	2.577	130.5	117.6	-	83.7	92.9	-	7.1	13.6	47.8
Average Volumetric Properties @ N_{des}											7.4	13.8	46.5

Blend	Sample ID		18-11829		P_b, %	3.5	G_{mm}	/1	2.752	/2	2.749	Avg	2.751
JMF	Dry Weight	Weight in H_2O	SSD Weight	G_{mb} @ $N_{compact}$	Height @ N_{ini}	Height @ N_{des}	Height @ N_{max}	$\%G_{mm}$ @ N_{ini}	$\%G_{mm}$ @ N_{des}	$\%G_{mm}$ @ N_{max}	VIM @ $N_{compact}$	VMA @ N_{des}	VFA @ N_{des}
Spec 1	5097.5	3152.6	5118.2	2.593	128.2	115.9	-	85.2	94.3	-	5.7	13.5	57.8
Spec 2	5095.4	3147.8	5118.7	2.585	129.2	117.0	-	85.1	94.0	-	6.0	13.7	56.2
Spec 3	5093.2	3150.6	5116.0	2.591	128.4	116.4	-	85.4	94.2	-	5.8	13.5	57.0
Average Volumetric Properties @ N_{des}											5.8	13.6	57.0

Blend	Sample ID		18-11830		P_b, %	4.0	G_{mm}	/1	2.726	/2	2.724	Avg	2.725
JMF	Dry Weight	Weight in H_2O	SSD Weight	G_{mb} @ $N_{compact}$	Height @ N_{ini}	Height @ N_{des}	Height @ N_{max}	$\%G_{mm}$ @ N_{ini}	$\%G_{mm}$ @ N_{des}	$\%G_{mm}$ @ N_{max}	VIM @ $N_{compact}$	VMA @ N_{des}	VFA @ N_{des}
Spec 1	5098.4	3162.0	5114.2	2.612	127.6	116.2	-	87.3	95.9	-	4.1	13.3	69.2
Spec 2	5089.1	3156.9	5103.6	2.614	128.0	115.8	-	86.8	95.9	-	4.1	13.2	68.9
Spec 3	5098.1	3161.2	5107.7	2.619	126.5	114.8	-	87.2	96.1	-	3.9	13.1	70.2
Average Volumetric Properties @ N_{des}											4.1	13.2	69.4

Blend	Sample ID		18-11831		P_b, %	4.5	G_{mm}	/1	2.704	/2	2.706	Avg	2.705
JMF	Dry Weight	Weight in H_2O	SSD Weight	G_{mb} @ $N_{compact}$	Height @ N_{ini}	Height @ N_{des}	Height @ N_{max}	$\%G_{mm}$ @ N_{ini}	$\%G_{mm}$ @ N_{des}	$\%G_{mm}$ @ N_{max}	VIM @ $N_{compact}$	VMA @ N_{des}	VFA @ N_{des}
Spec 1	5075.2	3148.2	5083.6	2.622	125.9	113.8	-	87.6	96.9	-	3.1	13.4	76.9
Spec 2	5078.2	3150.5	5086.0	2.624	126.1	114.1	-	87.8	97.0	-	3.0	13.3	77.4
Spec 3	5085.5	3150.3	5093.2	2.617	127.0	114.9	-	87.5	96.7	-	3.3	13.6	75.7
Average Volumetric Properties @ N_{des}											3.1	13.4	76.7

Blend	Sample ID		18-11832		P_b, %	5.0	G_{mm}	/1	2.678	/2	2.680	Avg	2.679
JMF	Dry Weight	Weight in H_2O	SSD Weight	G_{mb} @ $N_{compact}$	Height @ N_{ini}	Height @ N_{des}	Height @ N_{max}	$\%G_{mm}$ @ N_{ini}	$\%G_{mm}$ @ N_{des}	$\%G_{mm}$ @ N_{max}	VIM @ $N_{compact}$	VMA @ N_{des}	VFA @ N_{des}
Spec 1	5038.7	3124.4	5042.0	2.628	123.6	111.9	-	88.8	98.1	-	1.9	13.7	86.1
Spec 2	5083.4	3145.4	5084.5	2.622	124.8	113.3	-	88.9	97.9	-	2.1	13.9	84.9
Spec 3	5033.9	3118.3	5035.2	2.626	124.7	112.9	-	88.7	98.0	-	2.0	13.7	85.4
Average Volumetric Properties @ N_{des}											2.0	13.8	85.5

SUMMARY OF GYRATORY CURVE DATA							DESIGN ESTIMATE		
Binder Content	3.0	3.5	4.0	4.5	5.0	Specification	3.9	4.1	4.3
G_{mb} @ N_{des}	2.570	2.590	2.615	2.621	2.625		2.608	2.614	2.619
G_{mm}	2.775	2.751	2.725	2.705	2.679		2.731	2.722	2.712
VIM @ N_{ini}	16.2	14.8	12.9	12.4	11.2	> 11 %	13.5	13.0	12.5
VIM @ N_{des}	7.4	5.8	4.1	3.1	2.0	4 %	4.5	4.0	3.5
VMA @ N_{des}	13.8	13.6	13.2	13.4	13.8	≥ 13 %	13.3	13.3	13.3
VFA @ N_{des}	46.5	57.0	69.4	76.7	85.5	65 - 75	66.3	70.2	73.9
Dust to P_{be} Ratio	1.7	1.4	1.2	1.1	0.9	0.6 - 1.2	1.3	1.2	1.1

Prepared By: Zahi Chamoun
Project Engineer

س.ت : ١٦٥٢٢
الدوحة - قطر
C.R. : 16522
Doha-Qatar

Reviewed By: Quality Assurance /
Quality Control Dept.

C.R. No.: 16522, P.O. Box 47 167, Doha, Qatar, pavements.fme@fugro.com

V1R2 150405
11 of 18

Page 10

Figure B10. Mix Design Volumitric Data - 1

FUGRO PENINSULAR
Geotechnical, Material Testing, Engineers, Foundation Testing, Pavement Services

Pavements Services Division
Asphalt Mix Design Services

MIX DESIGN VOLUMETRIC DATA

JMF No.: QTR/119
Report No.: 00038

Plant:	MIDMAC COLAS	**Design ESAL:**	Not Applicable (N/A)
Designer:	Zahi Chamoun	**Asphalt Grade:**	PG 76E-10
Date:	07-Jan-19	**Aggregate Source:**	Village Trading Group
NMAS:	25.0 mm	**Asphalt Source:**	MEMBCO
Material Type:	Not Applicable (N/A)	**Binder Content:**	4.1%

Blend	Sample ID		18-11828	P_b, %	3.0	G_{mm}	/1	2.775	/2	2.774	Avg	2.775
JMF	Dry Weight	Weight in H_2O	SSD Weight	G_{mb} @ $N_{compact}$	Height @ N_{ini}	Height @ N_{des}	Height @ N_{max}	$\%G_{mm}$ @ N_{ini}	$\%G_{mm}$ @ N_{des}	$\%G_{mm}$ @ N_{max}	VIM @ $N_{compact}$	VMA @ N_{des}	VFA @ N_{des}
Spec 1	5092.1	3153.3	5140.7	2.562	129.5	117.5	-	83.8	92.3	-	7.7	14.1	45.4
Spec 2	5090.6	3153.6	5134.2	2.570	129.2	117.2	-	84.0	92.6	-	7.4	13.8	46.4
Spec 3	5097.2	3160.6	5138.2	2.577	130.5	117.6	-	83.7	92.9	-	7.1	13.6	47.8
Average Volumetric Properties @ N_{des}											7.4	13.8	46.5

Blend	Sample ID		18-11829	P_b, %	3.5	G_{mm}	/1	2.752	/2	2.749	Avg	2.751
JMF	Dry Weight	Weight in H_2O	SSD Weight	G_{mb} @ $N_{compact}$	Height @ N_{ini}	Height @ N_{des}	Height @ N_{max}	$\%G_{mm}$ @ N_{ini}	$\%G_{mm}$ @ N_{des}	$\%G_{mm}$ @ N_{max}	VIM @ $N_{compact}$	VMA @ N_{des}	VFA @ N_{des}
Spec 1	5097.5	3152.6	5118.2	2.593	128.2	115.9	-	85.2	94.3	-	5.7	13.5	57.8
Spec 2	5095.4	3147.8	5118.7	2.585	129.2	117.0	-	85.1	94.0	-	6.0	13.7	56.2
Spec 3	5093.2	3150.6	5116.0	2.591	128.4	116.4	-	85.4	94.2	-	5.8	13.5	57.0
Average Volumetric Properties @ N_{des}											5.8	13.6	57.0

Blend	Sample ID		18-11830	P_b, %	4.0	G_{mm}	/1	2.726	/2	2.724	Avg	2.725
JMF	Dry Weight	Weight in H_2O	SSD Weight	G_{mb} @ $N_{compact}$	Height @ N_{ini}	Height @ N_{des}	Height @ N_{max}	$\%G_{mm}$ @ N_{ini}	$\%G_{mm}$ @ N_{des}	$\%G_{mm}$ @ N_{max}	VIM @ $N_{compact}$	VMA @ N_{des}	VFA @ N_{des}
Spec 1	5098.4	3162.0	5114.2	2.612	127.6	116.2	-	87.3	95.9	-	4.1	13.3	69.2
Spec 2	5089.1	3156.9	5103.6	2.614	128.0	115.8	-	86.8	95.9	-	4.1	13.2	68.9
Spec 3	5098.1	3161.2	5107.7	2.619	126.5	114.8	-	87.2	96.1	-	3.9	13.1	70.2
Average Volumetric Properties @ N_{des}											4.1	13.2	69.4

Blend	Sample ID		18-11831	P_b, %	4.5	G_{mm}	/1	2.704	/2	2.706	Avg	2.705
JMF	Dry Weight	Weight in H_2O	SSD Weight	G_{mb} @ $N_{compact}$	Height @ N_{ini}	Height @ N_{des}	Height @ N_{max}	$\%G_{mm}$ @ N_{ini}	$\%G_{mm}$ @ N_{des}	$\%G_{mm}$ @ N_{max}	VIM @ $N_{compact}$	VMA @ N_{des}	VFA @ N_{des}
Spec 1	5075.2	3148.2	5083.6	2.622	125.9	113.8	-	87.6	96.9	-	3.1	13.4	76.9
Spec 2	5078.2	3150.5	5086.0	2.624	126.1	114.1	-	87.8	97.0	-	3.0	13.3	77.4
Spec 3	5085.5	3150.3	5093.2	2.617	127.0	114.9	-	87.5	96.7	-	3.3	13.6	75.7
Average Volumetric Properties @ N_{des}											3.1	13.4	76.7

Blend	Sample ID		18-11832	P_b, %	5.0	G_{mm}	/1	2.678	/2	2.680	Avg	2.679
JMF	Dry Weight	Weight in H_2O	SSD Weight	G_{mb} @ $N_{compact}$	Height @ N_{ini}	Height @ N_{des}	Height @ N_{max}	$\%G_{mm}$ @ N_{ini}	$\%G_{mm}$ @ N_{des}	$\%G_{mm}$ @ N_{max}	VIM @ $N_{compact}$	VMA @ N_{des}	VFA @ N_{des}
Spec 1	5038.7	3124.4	5042.0	2.628	123.6	111.9	-	88.8	98.1	-	1.9	13.7	86.1
Spec 2	5083.4	3145.4	5084.5	2.622	124.8	113.3	-	88.9	97.9	-	2.1	13.9	84.9
Spec 3	5033.9	3118.3	5035.2	2.626	124.7	112.9	-	88.7	98.0	-	2.0	13.7	85.4
Average Volumetric Properties @ N_{des}											2.0	13.8	85.5

SUMMARY OF GYRATORY CURVE DATA							DESIGN ESTIMATE		
Binder Content	3.0	3.5	4.0	4.5	5.0	Specification	3.9	4.1	4.3
G_{mb} @ N_{des}	2.570	2.590	2.615	2.621	2.625		2.608	2.614	2.619
G_{mm}	2.775	2.751	2.725	2.705	2.679		2.731	2.722	2.712
VIM @ N_{ini}	16.2	14.8	12.9	12.4	11.2	> 11 %	13.5	13.0	12.5
VIM @ N_{des}	7.4	5.8	4.1	3.1	2.0	4 %	4.5	4.0	3.5
VMA @ N_{des}	13.8	13.6	13.2	13.4	13.8	≥ 13 %	13.3	13.3	13.3
VFA @ N_{des}	46.5	57.0	69.4	76.7	85.5	65 - 75	66.3	70.2	73.9
Dust to P_{be} Ratio	1.7	1.4	1.2	1.1	0.9	0.6 - 1.2	1.3	1.2	1.1

Prepared By: Zahi Chamoun
Project Engineer

Reviewed By: Quality Assurance / Quality Control Dept.

C.R. No.: 16522, P.O. Box 47 167, Doha, Qatar, pavements.fme@fugro.com

V1R2 150405

Figure B11. Mix Design Volumitric Data - 2

FUGRO PENINSULAR

Geotechnical, Material Testing, Engineers,
Foundation Testing, Pavement Services

Pavements Services Division
Asphalt Mix Design Services

MIX DESIGN VOLUMETRIC DATA CURVES	JMF No.:	QTR/119
	Report No.:	00038

Plant:	MIDMAC COLAS	**Design ESAL:**	Not Applicable (N/A)
Designer:	Zahi Chamoun	**Asphalt Grade:**	PG 76E-10
Date:	07-Jan-19	**Aggregate Source:**	Village Trading Group
NMAS:	25.0 mm	**Asphalt Source:**	MEMBCO
Material Type:	Not Applicable (N/A)	**Binder Content:**	4.1%

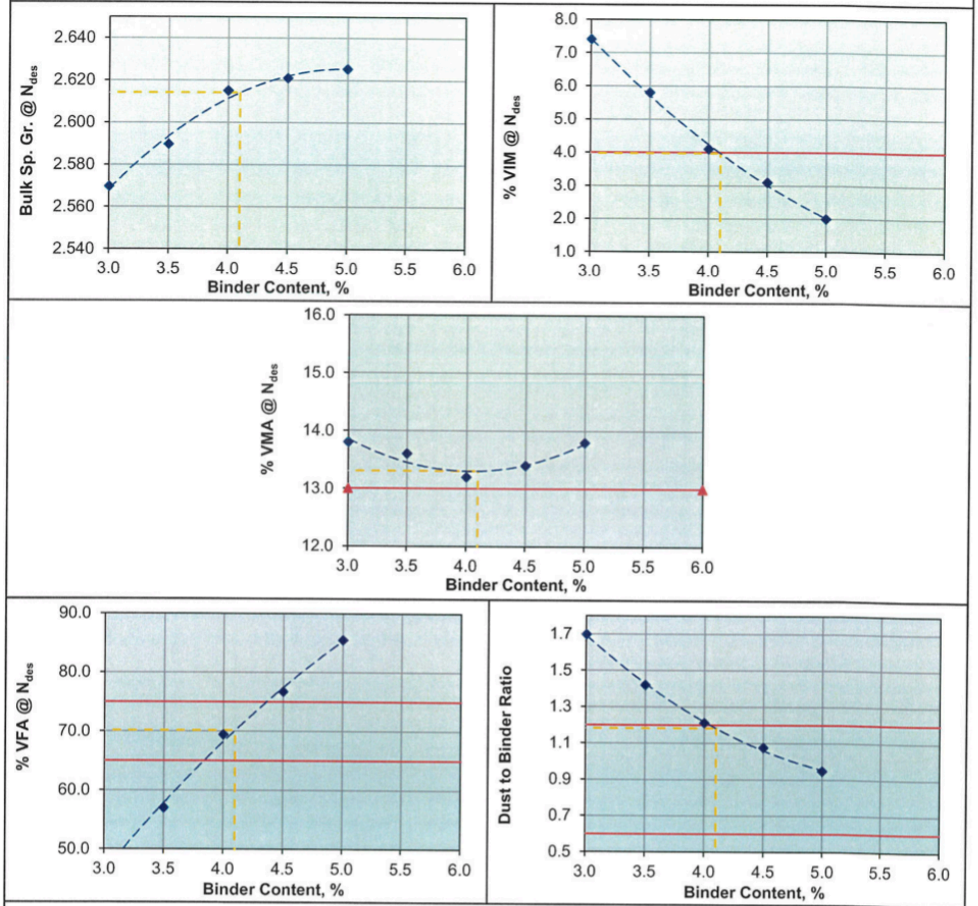

Prepared By: Zahi Chamoun
Project Engineer

Reviewed By: Quality Assurance /
Quality Control Dept.

C.R. No.: 16522, P.O. Box 47 167, Doha, Qatar, pavements.fme@fugro.com

V1R2 150405
12 of 18

Page 12

Figure B12. Mix Design Volumtric Data Curves

FUGRO PENINSULAR

Geotechnical, Material Testing, Engineers,
Foundation Testing, Pavement Services

Pavements Services Division
Asphalt Mix Design Services

FUGRO

DESIGN BINDER CONTENT VERIFICATION

JMF No.: QTR/119

Report No.: 00038

Plant: MIDMAC COLAS
Designer: Zahi Chamoun
Date: 07-Jan-19
NMAS: 25.0 mm
Material Type: Not Applicable (N/A)

Design ESAL: Not Applicable (N/A)
Asphalt Grade: PG 76E-10
Aggregate Source: Village Trading Group
Asphalt Source: MEMBCO
Binder Content: 4.1%

N_{des}=100 N_{max}=160	Sample ID		**18-12114**		Binder Content		**4.1**		G_{mm}	/1	2.723	/2	2.718	2.721
	Dry Weight	Weight in H_2O	SSD Weight	G_{mb} @ $N_{compact}$	Height @ N_{ini}	Height @ N_{des}	Height @ N_{max}	%G_{mm} @ N_{ini}	%G_{mm} @ N_{des}	%G_{mm} @ N_{max}	VIM @ N_{des}	VIM @ N_{max}	VMA @ N_{des}	VFA @ N_{des}
/1 N_{des}	5084.4	3152.1	5099.8	2.610	128.7	115.9	-	86.4	95.9	-	4.1	-	13.5	69.6
/2 N_{des}	5080.2	3151.2	5094.9	2.614	128.2	115.7	-	86.7	96.1	-	3.9	-	13.3	70.7
/3 N_{des}	5082.0	3150.7	5098.8	2.609	129.6	116.8	-	86.4	95.9	-	4.1	-	13.5	69.6
/4 N_{max}	5103.6	3184.5	5116.0	2.642	129.5	117.0	115.5	86.6	95.9	97.1	4.1	2.9	12.4	66.9
/5 N_{max}	5068.1	3160.1	5076.1	2.645	128.3	115.7	114.2	86.5	96.0	97.2	4.0	2.8	12.3	67.5
G_b	**1.03**	P_{ba}	0.4	P_{be}	3.7	F/A	1.2	Avg Vol Properties @ N_{des}			**4.0**	**-**	**13.4**	**70.0**
G_{sb}	**2.892**	G_{se}	2.926	G_{sa}	**2.892**	$P_{0.075}$	**4.4**	Avg Vol Properties @ N_{max}			-	**2.9**	-	-

SUMMARY OF GYRATORY VERIFICATION DATA

Design Parameter	Specification 25045-27-3PS-02401		Average Test Result 18-12114
N_{ini}, Avg VIM, %	> 11%		13.5
N_{des}, Avg VIM, %	4%		4.0
N_{des}, Avg VMA, %	> 13%		13.4
N_{des}, Avg VFA, %	65%	75%	70.0
N_{max}, Avg VIM, %	> 2%		2.9
$P_{0.075}/P_{be}$	0.6	1.2	1.2

BINDER CONTENT SELECTION

A design binder content of 4.1% was selected with the intention of balancing the target volumetric properties (VIM, VMA, and VFA at N_{design} and VIM at N_{max}).

Prepared By: Zahi Chamoun
Project Engineer

Reviewed By: Quality Assurance /
Quality Control Dept.

Figure B13. Design Binder Content Verification

FUGRO PENINSULAR

Geotechnical, Material Testing, Engineers,
Foundation Testing, Pavement Services

Pavements Services Division
Asphalt Mix Design Services

TENSILE STRENGTH RATIO (AASHTO T283)

JMF No.: QTR/119

Report No.: 00038

Plant:	MIDMAC COLAS	**Design ESAL:**	Not Applicable (N/A)
Designer:	Zahi Chamoun	**Asphalt Grade:**	PG 76E-10
Date:	07-Jan-19	**Aggregate Source:**	Village Trading Group
NMAS:	25.0 mm	**Asphalt Source:**	MEMBCO
Material Type:	Not Applicable (N/A)	**Binder Content:**	4.1%

VOLUMETRIC PROPERTIES OF TEST SPECIMENS

	Sample ID	18-12214						
	Sample Number	1	2	3	4	5	6	
t	Sample Height, mm	94.9	94.9	94.9	94.9	95.0	94.9	95 ± 5 mm
D	Sample Diameter, mm	150.0	150.0	150.0	150.0	150.0	150.0	
A	Dry Mass	3997.8	4011.9	4017.0	4009.1	4013.6	4015.4	
C	Mass in Water	2446.7	2443.9	2452.1	2453.7	2455.1	2462.9	
B	SSD Mass	4026.6	4034.2	4044.3	4036.4	4042.0	4043.5	
E	Volume of Sample (B - C), cc	1579.9	1590.3	1592.2	1582.7	1586.9	1580.6	
G_{mb}	Bulk Specific Gravity (A / E)	2.53	2.523	2.523	2.533	2.529	2.540	
G_{mm}	Maximum Density	2.721	2.721	2.721	2.721	2.721	2.721	
P_a	%VIM [100*(G_{mm} - G_{mb}) / G_{mm}]	7.0	7.3	7.3	6.9	7.1	6.7	7 ± 0.5 %
V_a	Vol. of Air Voids (P_a *E / 100), cc	110.6	116.1	116.2	109.2	112.7	105.9	

SATURATION OF CONDITIONED SPECIMEN SET

	Sample Number	1	2	3	4	5	6	
B'	SSD Mass after Saturation	-	-	-	4087.8	4098.9	4093.4	
C'	Mass in Water after Saturation	-	-	-	2505.7	2513.2	2510.3	
E'	Vol. of Sat. Sample (B' - C'), cc	-	-	-	1582.1	1585.7	1583.1	
J'	Vol. of Abs. Water (B' - A), cc	-	-	-	78.7	85.3	78.0	
S''	% Saturation (100*J' / V_a)	-	-	-	72.1	75.7	73.7	70 - 80 %

TENSILE STRENGTH RATIO RESULTS

	Sample Number	1	2	3	4	5	6	
P'	Recorded Load (@ 25ºC), N	15,989	13,977	15,471	14,696	14,517	15,047	
S	Indirect Tensile Strength, kPa	715.1	625.1	691.9	657.2	648.5	672.9	
	Average ITS for each set, kPa		677			660		
	CoV for each set, %		6.9			1.9		
	Tensile Strength Ratio (TSR), %				97			Specification > 80%

Prepared By: Zahi Chamoun
Project Engineer

Reviewed By: Quality Assurance / Quality Control Dept.

C.R.: 16522
Doha-Qatar
Fugro Peninsular

C.R. No.: 16522, P.O. Box 47 167, Doha, Qatar, pavements.fme@fugro.com

V1R2 150405
14 of 18

Page 14

Figure B14. Tensile Strength Ratio (AASHTO T283)

FUGRO PENINSULAR

Geotechnical, Material Testing, Engineers,
Foundation Testing, Pavement Services

Pavements Services Division
Asphalt Mix Design Services

FUGRO

DYNAMIC MODULUS OF LAB MIX (AASHTO TP79)

JMF No.: QTR/119
Report No.: 00038

Plant:	MIDMAC COLAS	**Design ESAL:**	Not Applicable (N/A)
Designer:	Zahi Chamoun	**Asphalt Grade:**	PG 76E-10
Date:	07-Jan-19	**Aggregate Source:**	Village Trading Group
NMAS:	25.0 mm	**Asphalt Source:**	MEMBCO
Material Type:	Not Applicable (N/A)	**Binder Content:**	4.1%
Prodcution Date:	20-Dec-18	**Trial Location:**	No Placement

Replicate ID	18-12214/3	18-12214/4	18-12214/7		Average	Std Dev
% VIM	6.1	6.0	6.1		6.1	0.1
% VMA	16.3	16.2	16.2		16.2	0.1
% VFA	62.5	62.8	62.6		62.6	0.2
Diameter (mm)	100.1	100.2	99.9		100.1	0.2
Height (mm)	150.5	150.9	150.5		150.6	0.2

Temp (ºC)	Freq (Hz)	Dynamic Modulus (MPa) /3	/4	/7	Phase Angle (º) /3	/4	/7	Modulus (MPa) Avg	CoV	Phase Angle (º) Avg	Std Dev
4	10	18,653	18,741	17,615	10.63	9.83	9.77	18,336	3.4	10.08	0.48
	1	13,981	14,433	13,555	13.77	12.84	12.59	13,990	3.1	13.07	0.62
	0.1	9,770	10,197	9,767	17.78	16.89	16.38	9,911	2.5	17.02	0.71
20	10	9,463	8,534	8,975	19.72	20.67	18.66	8,991	5.2	19.68	1.01
	1	5,694	4,963	5,600	24.52	25.72	23.35	5,419	7.3	24.53	1.19
	0.1	3,097	2,589	3,173	28.62	30.00	27.79	2,953	10.8	28.80	1.12
45	10	1,717	1,325	1,622	34.06	35.49	34.17	1,555	13.2	34.57	0.80
	1	763	541	708	31.60	32.71	32.78	671	17.2	32.36	0.66
	0.1	374	245	324	27.00	27.81	28.87	314	20.7	27.89	0.94
	0.01	236.5	144.7	180.3	21.33	22.62	24.03	187.2	24.7	22.66	1.35

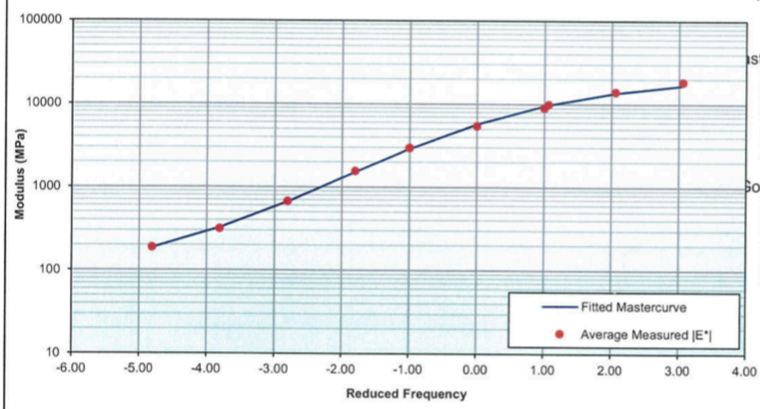

Reference Temp (ºC)

Ref T	20

ıster Curve Fit Parameters

δ	4.0132
β	-1.1675
γ	-0.58
ΔE_a	200583

ɜoodness of Fit Statistics

S_e	0.023
S_y	0.709
S_e/S_y	0.033
R^2	0.9990

Prepared By: Zahi Chamoun
Project Engineer

Reviewed By: Quality Assurance /
Quality Control Dept.

C.R. No.: 16522, P.O. Box 47 167, Doha, Qatar, pavements.fme@fugro.com

V1R2 150405
16 of 18

Page 15

Figure B15. Dynamic Modulus of Lab Mix (AASHTO TP79)